



# Beyond wind-sector management - Optimal wind farm operational planning for balancing fatigue damage and extending lifetime

Niklas Requate<sup>1,2</sup>, Lukas Vollmer<sup>1</sup>, and René Hofmann<sup>2</sup>

<sup>1</sup>Fraunhofer IWES, Bremerhaven, Germany

<sup>2</sup>TU Wien, Vienna, Austria

**Correspondence:** Niklas Requate (niklas.requate@iwes.fraunhofer.de)

**Abstract.** We present an optimization framework for long-term wind farm operation that balances fatigue loads and energy yield to extend turbine and farm lifetime. The approach plans per-turbine derating setpoints for discrete wind conditions using an engineering wake model and surrogate models for power and damage. We formulate the problem as a nonlinear program and solve it either for the full farm in a single run or iteratively per turbine. The method is demonstrated on a 9-turbine farm under onshore and offshore turbulence conditions and across multiple failure modes. For tower bottom bending, modest lifetime extensions of 2–5 years increase net present value (NPV) between (5 % and more than 100 %) with small losses of annual energy production (AEP) of 1–4 % onshore and less than 0.2 % offshore. The per-turbine optimization achieves similar results as the full farm approach in most cases. Under offshore turbulence, upstream derating more effectively reduces wake-induced turbulence and the coordinated farm optimization yields additional benefits. When blade edgewise loads are included, lifetime gains require stronger derating due to rotational-speed sensitivity and reduce economic benefits. The framework produces implementable lookup tables that can be integrated into wind farm planning and control. While results rely on steady wake models and design-style damage estimation and thus represent first-order comparisons, they show that targeted derating can redistribute damage and extend lifetime with limited impact on energy.

## 1 Introduction

In wind farms, the wake effect has two negative effects: Reduced energy production due to lower wind speeds, and increased loads, due to higher turbulence. Both energy and loads can be influenced by control at the affected turbine or at neighboring turbines. For energy, the objective is clear: maximize farm-level annual energy production (AEP). For loads, the challenge is greater because energy production inevitably induces fatigue on multiple components. In contrast, optimizing loads presents a greater challenge as energy production unavoidably induces fatigue loads on various components of each turbine. Although standard methods like Miner's rule can estimate the impact of loads on the lifetime of structural components, these estimates are often associated with significant uncertainty. Nevertheless, it is clear that turbines exposed to wakes more frequently experience higher loads over their lifetime than other turbines. In every wind farm, the lifetime fatigue damage of each turbine needs to remain below the design fatigue budget, which is usually the same for each turbine and is defined by standards. If the fatigue budget is exceeded for some turbines of the farm during their nominal operation, some wind farms are required to apply sector



management and shut-down turbines in certain wind directions at the cost of a significant energy loss. By using derating<sup>1</sup> as an instrument for load reduction of individual turbines and full wind farms, the opportunity to redistribute fatigue damage for different inflow conditions opens. Using this, wind farm operation can be optimized to extend wind farm lifetime and to maximize revenue. According to BDEW (2025), longer wind farm operation also has macroeconomic benefits for society.

To place this work, we focus on wind farm flow control and load reduction at farm level, and on methods for long-term operational planning. Research into wind farm control has grown significantly in recent years, with numerous studies focusing on strategies to optimize power production and reduce structural fatigue. Several overview papers summarize these advancements, including works by Houck (2022); Nash et al. (2021); Kölle et al. (2022); Meyers et al. (2022); Eguinoa et al. (2021). Previous research in wind farm control has predominantly emphasized maximizing power generation at the farm level by mitigating wake effects. A distinction between wind farm flow control, summarizing techniques for wake mitigation, and wind farm power plant control (WPPC) was introduced in Eguinoa et al. (2021).

WPPC focuses on the interface of the wind farm with the power grid which is not covered within this work. Despite that the maximization of power production comes with its own challenges mentioned in the literature above, the explicit focus on damage distribution and lifetime has a few major disadvantages and additional complications. On the one hand, it is required to use additional models for the influence of the parameters on the different components. In the context of farm flow optimization and control, this is often addressed through surrogate models. On the other hand, the power maximization problem can be divided into simplified subproblems because the annual energy production can be maximized by maximizing the power production under each separate condition. Turbine lifetime is determined by the cumulative damage accumulated under various operating conditions. Consequently, dividing the optimization process into smaller independent problems leads to suboptimal results.

In several studies on wind farm flow control, load reduction or lifetime of the turbines is considered, but only considered as a side objective or constraint. In Gharbia et al. (2025), the complexity of the full optimization approach for turbine lifetime is explicitly discussed. Therefore, they also perform a bin-wise optimization under local load constraints followed by an a posteriori check of the global lifetime damage equivalent loads (DELs). The global approach proved to be too time-consuming for their study with 15 turbines and a high resolution of the selected bins. In Liew et al. (2024), it was possible to consider lifetime DELs as global constraints when maximizing AEP. The resolution of bins, and thus the size of the optimization problem, remain unclear. Unlike in this work, both studies use yaw misalignment and derating as control instruments. Both studies highlight optimization approaches that are directly related to our work and underscore the need for further research in this area.

Various studies have also examined the role of derating strategies as a means to manage loads in wind farms and their impact on downstream turbines. For instance, Astrain Juangarcia et al. (2018) and Meng et al. (2020) demonstrate that reducing the thrust of upstream turbines can be used to reduce loads at downstream turbines. More recently, Guilloré et al. (2024) presented an approach for control oriented surrogate models for wind farms for both wake-steering and derating applications. Such

---

<sup>1</sup>In general, there are various terms for reducing the power of a wind turbine and the usage often depends on the context. In wind farm control, the term axial-induction control is often used. Also, down-regulation or curtailment are prominent terms. The latter is often referred to in the context of requests by the grid operator. Just like in Requate and Meyer (2023), the term derating is used throughout this work.



methods can be applied to improve accuracy of wind farm optimization approaches. Pettas and Cheng (2024) investigated the combined use of derating, power-boost strategies, and individual pitch control to optimize wind farm operation. They further applied these approaches in the context of electricity price optimization to improve economic outcomes (Pettas and Cheng, 2024). However, derating poses certain challenges. For example, Robbelein et al. (2023) highlighted that it can induce negative effects on the loads experienced by the tower or substructure, particularly for offshore wind turbines, due to reduced negative damping. To address this, Ziegler et al. (2024) proposed optimizing curtailment intervals to mitigate such risks effectively. Moreover, Condition Monitoring System (CMS) technology, as demonstrated by Pacheco et al. (2025), provides improved tools for assessing the blade-specific impacts of derating strategies in field applications.

In the context of wind farm control, derating is mainly applied for active power tracking when the farm power needs to be limited. In this case, the derating can be distributed among the turbines of the farm and influence loads in different ways (Jensen et al., 2016; Gonzalez Silva et al., 2023; Stock et al., 2020), but it is only applicable when the farm needs to be curtailed for a lifetime balancing of the farm. Derating is explicitly used for lifetime optimization of a wind farm in the commercial software WindPro (International, 2025). Here, a heuristic optimization process is used to reduce the fatigue damage below a certain level. The controller setpoints (or modes) are iteratively reduced under the wind conditions where it is most favorable for the damage-energy relationship (EMD International, 2025). With that approach, the energy yield of the farm is only maximized indirectly and an improved solution, but not necessarily the optimal one, might be found.

In Requate and Meyer (2023), we presented a mathematical optimization method to distribute the fatigue damage of a single turbine within a wind farm. However, the impact of modified control behavior through derating on other turbines was not yet considered. Building on this foundation, the method has now been expanded to optimize damage distribution across an entire wind farm, addressing wake-induced interactions between turbines. Since turbine loads are influenced by both individual operation and wake effects from neighboring turbines, this optimization addresses the interface between turbine and wind farm control. Requate and Meyer (2023) introduced the concept of integrating turbine fatigue management into farm-level control. Meyer and Requate (2023) expanded this idea by embedding long-term operational planning into a multi-layered system-wide wind farm control paradigm.

This work introduces an optimization framework to find operational strategies for wind farm operation that enables a system-wide optimized damage distribution for all turbines of a wind farm. It specifically employs derating not only as a strategy to extend the operational lifetime of wind turbines within a farm but also to balance fatigue damage across the turbines, thereby equalizing their overall value. The framework handles different layouts, site-specific conditions and constraints, and multiple failure modes. In practice, the choice of failure modes and target fatigue budgets or lifetimes depends on site assumptions, parameters, and operator preferences.

Within this work, we demonstrate the approach on an exemplary 9-turbine wind farm in onshore and offshore turbulence conditions on different failure modes. For each of these two conditions, we first consider the tower bottom bending moment (tower bm) as the relevant failure mode. This choice is taken, because the tower is a component which is usually not replaced and thus decisive for the full lifetime of a turbine. Subsequently, three failure modes are considered for the optimization process under Offshore-turbulence conditions. Because the optimization problem in a wind farm with many turbines can become very



large, we compare two approaches for all the cases mentioned. In addition to a coordinated solution for the entire wind farm, we investigate an iterative approach in which each turbine is optimized separately. We show that the coordinated approach is particularly effective under offshore conditions when turbulence in the wake is significantly increased.

95 At first, a general optimization problem for the operational planning of wind farms under given constraints on the fatigue budget is presented in Sect. 2. Then, the proposed approaches for the derating optimization are presented in Sect. 3. In Sect. 4, results for each of the three cases are presented. They are discussed in Sect. 5. A conclusion is given in Sect. 6.

## 2 General optimization problem for the operational planning of wind farms

We formulate a nonlinear optimization problem to find an operational plan for arbitrary wind farms. An operational plan is a set  
 100 of control setpoints to be applied under specific external (ambient) conditions. In this work, the external conditions are ambient wind conditions; the plan exploits the nonlinear relationship between energy yield and damage. In Requate and Meyer (2023), a four-step process for optimal operational planning of a single turbine was introduced. Here, we extend the system boundary to the entire farm and develop a method that produces an operational plan for each turbine, accounting for wake interactions.

The optimization problem is constructed to select an optimal control setpoint for each combination of selected input condi-  
 105 tions. The result of the optimization process is a lookup table that a wind farm control system can follow. The selection and discretization of input conditions strongly influence the setup of the optimization problem because they determine the number of decision variables (the setpoints to be selected). Total fatigue damage is computed using a discrete representation of average input conditions and their expected frequency of occurrence during the lifetime of a wind turbine. Thus, constructing the optimization problem for fatigue-damage planning begins with the selection of input conditions and discretizing them into bins  
 110 where the term bin is defined as an interval between two values as commonly used for statistical distributions. Subsequently, objectives and constraints are specified once the required surrogate models for fatigue damage and power production have been created (Steps 1 and 2 in Requate and Meyer (2023)). In Tables 1 and 2 we describe the required notation for the indices and input variables when setting up the optimization problem in a general way.

We use these variables to describe the wake interaction and the surrogate models, which are then used to set up the problem.

### 115 2.1 Wake modeling

The ambient-bin matrix  $X^{\text{amb}}$  and control plan  $U$  jointly determine local (at-turbine) wind conditions via an engineering wake model (FOXES, (Schmidt, 2022)). The wake model computes  $f^{\text{wake}}$  steady-state values  $x(u)$  for wind speed and turbulence intensity (TI). We denote the mapping for local wind condition  $X(U)$  by

$$\mathbf{X}(U) = f^{\text{wake}}(X^{\text{amb}}, U) \in \mathbb{R}^{N_T \times B \times w}. \quad (1)$$

120 Per ambient bin, turbines are coupled through wakes, and each bin is evaluated independently by the wake model. With a total number of bins  $B$  and a number of turbine  $N_T$ , the per-turbine local wind conditions are computed by:

$$x_{ij}(U) = \mathbf{X}(i, j, :) = f^{\text{wake}}(x_j^{\text{amb}}, U(i, j, :)), \quad i = 1, \dots, N_T, \quad j = 1, \dots, B. \quad (2)$$



Name	Notation	Example
Ambient input vector $x^{\text{amb}}$	$x^{\text{amb}} = (x^{(\text{amb},1)}, \dots, x^{(\text{amb},W)}) \in \mathbb{R}^W$ .	$W = 3$ : mean wind direction $\theta^{\text{amb}}$ , mean wind speed $v^{\text{amb}}$ , turbulence $TI^{\text{amb}}$ ; $x^{\text{amb}} = (\theta^{\text{amb}}, v^{\text{amb}}, TI^{\text{amb}})$
Matrix of ambient bin representatives $X^{\text{amb}}$	$X^{\text{amb}} \in \mathbb{R}^{B \times W}$ stores representative ambient vectors $x_j^{\text{amb}}$ in row $j$ .	With $B = B_\theta \cdot B_v \cdot B_{TI} = 36 \cdot 20 \cdot 1 = 720$ , $W = 3$ : shape $720 \times 3$ ; e.g., $x_0^{\text{amb}} = (0^\circ, 8.0 \text{ m/s}, 0.08 \text{ pu})$ , $x_2^{\text{amb}} = (10^\circ, 8.0 \text{ m/s}, 0.08 \text{ pu})$
Local (at-turbine) conditions $x$	$x = (x^{(1)}, \dots, x^{(w)}) \in \mathbb{R}^w$ .	$w = 3$ : mean wind direction $\theta$ , mean wind speed $v$ , turbulence intensity $TI$ ; $x = (\theta, v, TI)$
Tensor of local wind conditions $\mathbf{X}$	$\mathbf{X} \in \mathbb{R}^{N_T \times B \times w}$ stores local per-turbine wind conditions; per-turbine, per-bin vector $x_{ij} = \mathbf{X}(i, j, :)$ .	Example: $x_{0,0} = (0^\circ, 7.5 \text{ m/s}, 0.12 \text{ pu})$ at $x_0^{\text{amb}} = (0^\circ, 8.0 \text{ m/s}, 0.08 \text{ pu})$
Control setpoints $u(x)$	For each local condition $x$ , the controller applies setpoints $u(x) \in \mathbb{R}^{N_u}$ .	With $N_u = 2$ : derating factor $\delta^P$ and yaw misalignment $y$ ; $u(x) = (90\%, +5^\circ)$
Operational plan tensor $U$	$U \in \mathbb{R}^{N_T \times B \times N_u}$ , entries $u_{ijm}$ . For $N_u = 1$ (derating only), $U \in \mathbb{R}^{N_T \times B}$ with entries $u_{ij}$ .	With $N_T = 3$ , $B = 12$ , $N_u = 2$ : shape $3 \times 12 \times 2$ ; With $N_u = 1$ : derating value for turbine $i = 1$ at ambient bin $j = 0$ : $u_{1,0} = 90\%$ at $x_0^{\text{amb}} = (0^\circ, 8.0 \text{ m/s})$

**Table 1.** Notation and examples for variables

Name	Notation
Number of selected ambient variables	$W \in \mathbb{N}$
Number of selected local variables	$w \in \mathbb{N}$
Number of bins for ambient variable $x^{(\ell)}$	$B_{x^{(\ell)}} \in \mathbb{N}$
Total number of bins	$B = \prod_{\ell=1}^W B_{x^{(\ell)}} \in \mathbb{N}$
Number of turbines	$N_T \in \mathbb{N}$
Number of control channels	$N_u \in \mathbb{N}$
Turbine index	$i \in \{1, \dots, N_T\}$
Ambient-bin index	$j \in \{1, \dots, B\}$
Control-channel index	$m \in \{1, \dots, N_u\}$

**Table 2.** Notation for dimensions and indices

Given  $x_{ij}(U)$ , at-turbine damage and power can be computed using surrogate models implemented as turbine models in FOXES.



## 125 2.2 Surrogate models and lifetime metrics

We assume surrogate models for per-hour damage rate  $d_{\text{fm}}(x, u)$  for failure mode  $\text{fm}$  and for power  $P(x, u)$ , both as functions of local conditions  $x$  and control setpoint  $u$ . For simplicity, all turbines share the same surrogate models, though per-turbine models are possible. Both  $x$  and  $u$  depend on ambient conditions via Eq. (2).

130 The lifetime frequency vector over ambient bins is  $h \in \mathbb{R}^B$  with elements  $h_j \geq 0$  and  $\sum_{j=1}^B h_j = H_{\text{total}}$ . Alternatively, using probabilities  $p = (p_1, \dots, p_B) \in \mathbb{R}^B$  with  $\sum_{j=1}^B p_j = 1$  and a horizon  $H$ , one may replace  $h_j$  by  $H p_j$ .

The lifetime energy production of turbine  $i$  under plan  $U$  is

$$E_i(U; h) = \sum_{j=1}^B P(x_{ij}(U), u_{ij}) h_j, \quad (3)$$

and the lifetime damage of turbine  $i$  for failure mode  $\text{fm}$  is

$$D_{\text{fm},i}(U; h) = \sum_{j=1}^B d_{\text{fm}}(x_{ij}(U), u_{ij}) h_j. \quad (4)$$

135 In each wind-condition bin, control setpoints and local wind conditions are interdependent and are computed by FOXES for all turbines via an internal iteration process. This process can be performed for all bins  $j$  in parallel. The aggregate values of energy production and fatigue damage are then used to find an optimal operational plan under the expected average occurrence for each input condition.

## 2.3 General optimization problem

140 We seek an operational plan  $U$  that maximizes an objective  $F : \mathbb{R}^{N_T \times B \times N_u} \rightarrow \mathbb{R}$  (e.g., total energy) subject to per-turbine damage budgets  $D_{\text{fm},i}^{\text{target}}$  for selected failure modes  $\text{fm} \in \mathcal{F}$ :

$$\begin{aligned} \max_U \quad & F(U; h) \\ \text{s.t.} \quad & D_{\text{fm},i}(U; h) \leq D_{\text{fm},i}^{\text{target}}, \quad \forall i \in \{1, \dots, N_T\}, \forall \text{fm} \in \mathcal{F}, \\ & u_{ijm} \in [u_{\min}, u_{\max}] \quad \text{for all } i, j, m. \end{aligned} \quad (5)$$

For maximizing energy production, we use the objective function

$$F(U; h) = \sum_{i=1}^{N_T} E_i(U; h). \quad (6)$$

145 The optimization problem Eq. (5) is a large-scale nonlinear program (NLP). Nonlinearity arises from aerodynamic wake interactions and fatigue damage surrogate models  $d_{\text{fm}}(x, u)$  and we cannot assume convexity. The number of decision variables scales as  $N_T B N_u$  with  $B = \prod_{\ell} B_{x(\ell)}$ , so even moderate discretizations of wind direction and speed lead to thousands of variables. For calculating the wind farm wake effects, the ambient conditions at least contain the wind direction  $\theta$  and wind speed  $v$  as ambient variables. With a bin width of  $10^\circ$  for  $\theta^{\text{amb}}$  and 1 m/s for  $v^{\text{amb}}$  in a wind speed range from 5 m/s to



150 25 m/s, this results in  $B = 36 \cdot 20 = 720$  bins, i.e., almost 6500 variables in a 9-turbine farm and 72000 in an offshore farm with 100 turbines when only one control variable is used. Thus, the problem needs to be reduced in complexity, and dedicated solvers selected.

## 2.4 Economic evaluation of results

When solving the optimization problem in Eq. (5) to maximize energy production (Eq. (6)), we determine the maximum  
 155 amount of energy production under the constraints for a target fatigue budget. In other words, a trade-off between lifetime and energy production is found and different target values for the lifetime can be selected. We evaluate strategies economically using the net present value NPV with constant average price, capital and operating expenditure (CAPEX and OPEX), and weighted average cost of capital (WACC), following Requate and Meyer (2023) and adapting it to the farm level.

We need to define the lifetime of the full wind farm dependent on the selected operational plan. To do so, we assume that the  
 160 wind farm's lifetime ends when the first turbine reaches its target fatigue budget, i.e. when  $D_{\text{fm},i}(U;h) \geq 1$ . Thus, the lifetime of each turbine for a specific failure mode is given by

$$\tau_{\text{fm},i}(U;h) = \frac{25}{D_{\text{fm},i}(U;h)} \quad (7)$$

and the full number of operating years is given by

$$Y^{\text{life}} = \left\lfloor \min_{\text{fm} \in \mathcal{F}, i \in \{1, \dots, N_T\}} \tau_{\text{fm},i}(U;h) \right\rfloor. \quad (8)$$

165 This assumption allows for a straightforward comparison of the operational plans of full wind farms, but depends on strong deterministic assumptions about the end of life. Thus, it can only be used as a first indicator for the selection and evaluation of the operational plans.

The NPV over a horizon of  $Y$  years is computed as:

$$\text{NPV}(Y) = \sum_{t=0}^Y \frac{C_{\text{elPrice}} \cdot E^{\text{annual}}(U;h) - C_{\text{OPEX}}}{(1 + C_{\text{WACC}})^t}, \quad (9)$$

170 with constant parameters for the interest rate  $C_{\text{WACC}}$  covered by the WACC, constant annual maintenance costs  $C_{\text{OPEX}}$  and a constant average price of electricity  $C_{\text{elPrice}}$ . The repayment can be variable over the entire operating period and is made depending on the annual energy yield  $E^{\text{annual}}(U;h) := \frac{E(U;h)}{Y^{\text{life}}}$ .

## 3 Optimization problem for optimal planning of derating

Within this study, an optimized operational plan using derating setpoints of the wind turbines is found. The specific variables  
 175 and parameters for the presented use case are described in the Sect. 4. At this stage, the general problem is reduced to the required parameters for solving the derating problem. Subsequently, the iterative approach for solving the optimization problem for each turbine of the farm separately is introduced. The processes for both of the approaches are shown in Fig. 1 (denoted as full farm optimization) and Fig. 2 (denoted as per-turbine optimization). Finally, the implementation of both algorithms is described.



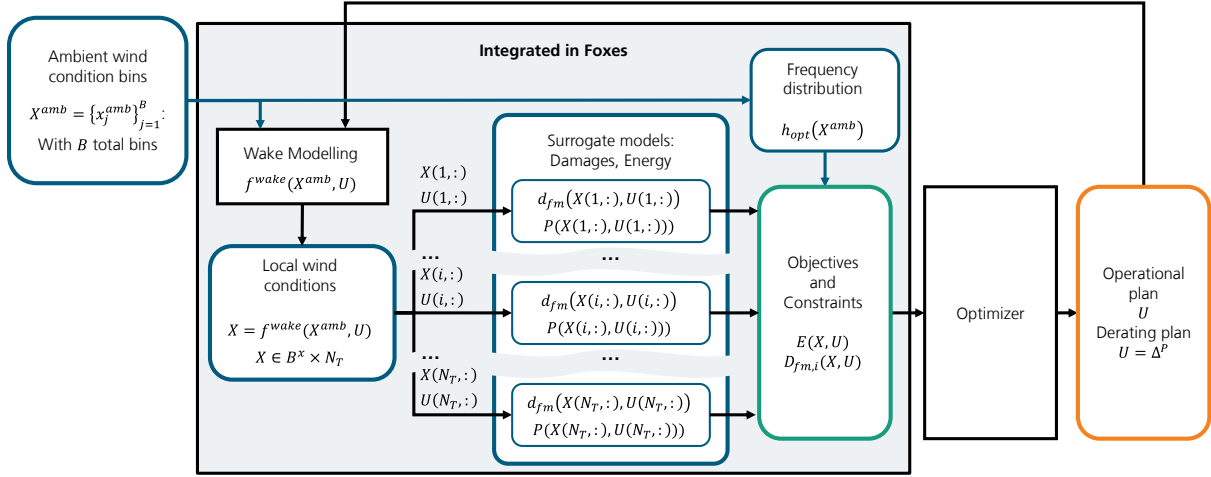


**Figure 1.** Process for full farm optimization in single run

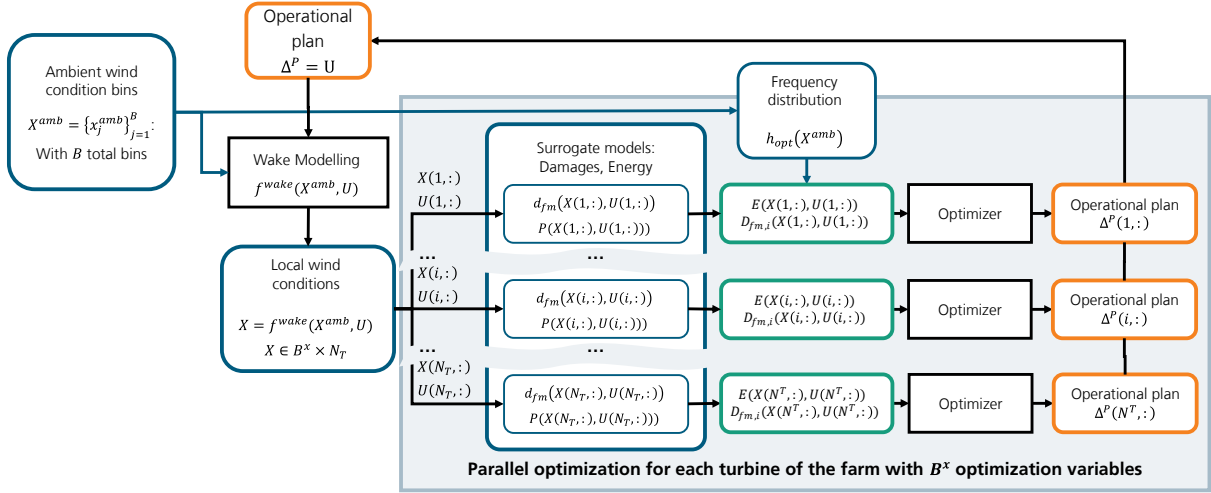


**Figure 2.** Process for iterative per-turbine optimization

### 180 3.1 Final formulation for single optimization run

The surrogate damage models depend on the local wind speed  $v$  and turbulence intensity  $TI$ , i.e.  $x = (v, TI)$ , as well as on a derating control setpoint  $u = \delta^P$ . Local conditions are computed from ambient values for wind direction  $\theta^{amb}$ , wind speed  $v^{amb}$ , turbulence intensity  $TI^{amb}$ , and air density  $\rho$ . The parameter  $\rho$  is kept constant and  $TI^{amb}$  may be treated as a function of wind speed. The derating setpoint  $\delta^P$  reduces power by a percentage amount at all wind conditions. The full operation plan for the wind farm (derating-only) is denoted as  $\Delta^P$  consistent with  $U$ . With this setup, we seek

$$- x_{ij}(\Delta^P) = f^{wake}(x_j^{amb}, \Delta^P(:, j)), \forall j = 1, \dots, B.$$





$$\begin{aligned} - B &= B_{\theta \text{amb}} B_{v \text{amb}}. \\ - U &= \Delta^P \in \mathbb{R}^{N_T \times B}. \end{aligned}$$

and the optimization problem

$$\begin{aligned} \max_{\Delta^P} \quad & E(\Delta^P; h) = \sum_{i=1}^{N_T} E_i(\Delta^P; h) \\ \text{s.t.} \quad & D_{\text{fm},i}(\Delta^P; h) \leq D_{\text{fm},i}^{\text{target}}, \quad \forall i \in \{1, \dots, N_T\}, \forall \text{fm} \in \mathcal{F}, \\ & \delta_{ij}^P \in [\delta_{\min}^P, \delta_{\max}^P] \text{ for all } i, j. \end{aligned} \tag{10}$$

The problem in Eq. (10) yields a single derating per turbine for each combination of wind speed and wind direction. Thus, the number of optimization variables depends on the number of bins  $B_{\theta \text{amb}}$  and  $B_{v \text{amb}}$  and on the number of turbines.

When using the frequency distribution over wind bins, some combinations of wind speed and wind direction are very rare. To reduce the number of variables with negligible influence on the objective and constraints, we removed the selected conditions from the optimization variables by testing their influence on the fatigue damage. All values, for which the maximum change in fatigue damage over all turbines and failure modes is less than 3%, are excluded. These are later set to the nominal power setpoint of 100% (no derating) automatically. In addition, power setpoints are rounded to integer values after the continuous optimization process to obtain realistic setpoints for a wind farm control algorithm. The effect on the results is negligibly small.

An overview of the setup of the optimization problem is given in Fig. 1.

### 3.2 Iterative loop optimizing separately for each turbine with derating

Since derating primarily affects the derated turbine and influences the wake only indirectly via reduced thrust, we investigate whether comparable results can be achieved when each turbine is optimized separately. This approach is easily scalable to large wind farms because each per-turbine problem has  $B$  variables and the problems can be solved in parallel. To include wake effects, we use an iterative procedure that optimizes each turbine's plan while holding the current local wind condition fixed, then updates them after each iteration. An overview of the loop approach is shown in Fig. 2 and described in Algorithm 1.

### 3.3 Implementation and selection of solvers

The problem is set up using an internally developed Python framework VIOLA (Value Integrated Optimization of Lifetime Asset Operation) which integrates all the required steps from building up the problem with suitable surrogate models, the integration of those models into the wake modeling tool FOXES up to the solution of the problem with dedicated solvers and the evaluation of results. For this study, the framework was enhanced with the integration of the fatigue damage models into FOXES and the subsequent setup of the optimization problem for a full wind farm. In addition, the loop iteration approach was implemented. For the high-dimensional, nonlinear problem (NLP), the gradient-based interior point solver IPOPT was selected (Wächter and Laird, 2022). Despite the lack of analytical gradients, the nonlinear, but differentiable behavior of the fatigue




---

**Algorithm 1** Iterative loop optimizing separately for each turbine with derating (using  $\Delta^P$ ), graphically represented in Fig. 2

---

```

1: Initialization: Start from a nominal plan  $\Delta^{P,(0)}$  (e.g., 100% power in all bins) and compute initial local conditions  $\mathbf{X}^{(0)} = f^{\text{wake}}(X^{\text{amb}}, \Delta^{P,(0)})$ .
2: for  $k = 1$  to  $K$  do
3:   Iterative loop (k): Given  $\Delta^{P,(k-1)}$ , recompute local conditions  $\mathbf{X}^{(k)} = f^{\text{wake}}(X^{\text{amb}}, \Delta^{P,(k-1)})$ ; denote local vectors by  $x_{ij}^{(k)} := \mathbf{X}^{(k)}(i, j, :) \in \mathbb{R}^w$ .
4:   for  $i = 1$  to  $N_T$  do
5:     For turbine  $i$ , solve its per-turbine problem over bins  $j = 1, \dots, B$ :
6:     maximize  $\sum_{j=1}^B P(x_{ij}^{(k)}, \delta_{ij}^P) h_j$ 
7:     subject to  $\sum_{j=1}^B d_{\text{fm}}(x_{ij}^{(k)}, \delta_{ij}^P) h_j \leq D_{\text{fm},i}^{\text{target}}$  for all  $\text{fm} \in \mathcal{F}$ 
8:     and  $\delta_{ij}^P \in [\delta_{\min}^P, \delta_{\max}^P]$  for all  $j$ 
9:     Update the  $i$ -th row of  $\Delta^{P,(k)}$  with the optimizer's solution.
10:  end for
11: end for
12: Return the final plan  $\widehat{\Delta}^P \leftarrow \Delta^{P,(K)}$  and  $\widehat{\mathbf{X}} \leftarrow f^{\text{wake}}(X^{\text{amb}}, \widehat{\Delta}^P)$ .
```

---

215 damage models and the scalability to a large number of optimization variables led to this choice. In contrast, deterministic global optimization (e.g., branch-and-bound with convex relaxations) and metaheuristics (e.g., evolutionary algorithms, particle swarm optimization) generally scale poorly with dimension due to the exponential growth of the search space and large numbers of function evaluations. With IPOPT, the problem could be solved within reasonable time for the selected problem size.

## 4 Results

220 The proposed method is applied for different wind farm scenarios with 7.5 MW wind turbines (rotor diameter: 164 m, hub height: 100 m) using the simulation database as described in Requate et al. (2022), available on Zenodo (Requate and Meyer, 2023). The example wind farm consists of 9 turbines with a regular  $3 \times 3$  layout and the wind comes mainly from the southwest (see Fig. 3). The frequency distribution of wind speed is computed from a 30-year time series of ERA5 data in the German North Sea (Hersbach et al., 2018). The utilized terms and parameters for the damage models are summarized in Table 3. For the

225 wake models in FOXES, the local wind speed is computed using the Gauss-type wake model by Bastankhah and Porté-Agel (2016). The wake-induced TI is calculated using the top-hat wake model as described in IEC (2019a). For the wind speed, a quadratic superposition is used, and TI is superposed using the maximum rule.

As explained in Sect. 2, the binning of ambient wind conditions is a key design choice because it determines the number of optimization variables. A compromise between computational effort and accuracy is required, and the granularity should

230 remain implementable for the usage of the setpoints on real turbines. To assess this trade-off, we computed total energy and damage (Eq. (3) and Eq. (4)) for several discretizations. In addition, the optimization was first tested with coarser discretizations and then refined. With a bin width of  $10^\circ$  for ambient wind direction and 3 m/s for wind speed, results were obtained in



**Table 3.** Summary of terms for the selected failure modes

Load	Flapwise Bending Moment	Edgewise Bending Moment	Tower Bottom Bending Moment
Abbreviation	Flapwise bm	Edgewise bm	Tower (bottom) bm
Wöhler Exponent	10	10	3
Damage Rate	$d_{flap}(x, u)$ [1/h]	$d_{edge}(x, u)$ [1/h]	$d_{tower}(x, u)$ [1/h]

reasonable time and the relative changes in annual energy and resulting lifetime were close to the finest tested discretization (using  $3.3^\circ$  and  $1 \text{ m/s}$ ).

235 The total frequency for both distributions is shown in Fig. 3. For the evaluation, we use the fine discretization to evaluate the results and include a sensitivity to the coarser discretization. TI is handled as a single value depending on the wind speed to keep problem size manageable; this also reflects practical limitations of the TI values which are difficult to measure in reality and thus less suitable as input for a control setpoint. The parameters for both binnings are summarized in Table 4. The number of ambient bins  $B_{opt}$  is reduced by about 10% for all use cases by removing low frequent conditions as described in Sect. 3.

240 This mainly applies to wind speeds of  $22 \text{ m/s}$  in some north-western wind directions.

**Table 4.** Binning parameters for optimization (coarse) and evaluation (fine).

Variable	Optimization binning (coarse)	Evaluation binning (fine)
Wind direction $\theta$	$B_{\theta}^{opt} = 36$ , bin width $10^\circ$ ; centers $0, 10, \dots, 350^\circ$	$B_{\theta}^{eval} = 108$ , bin width $\frac{10}{3} \approx 3.3^\circ$ ; centers $0, 3.3, \dots, 356.7^\circ$
Wind speed $v$	$B_v^{opt} = 6$ , bin width $3 \text{ m/s}$ ; centers $7, \dots, 10, 22 \text{ m/s}$	$B_v^{eval} = 20$ ; bin width $1 \text{ m/s}$ ; example centers $5, 6, \dots, 24 \text{ m/s}$
Turbulence intensity TI	$B_{TI}^{opt} = 1$ ; single value; dependent on $v$	$B_{TI}^{eval} = 1$ ; single value; dependent on $v$
Total number of ambient bins	$B^{opt} = 216$	$B^{eval} = 2160$
Frequency per wind condition	$h^{opt}$	$h^{eval}$

In different subsections, we present results for the different use-cases with ambient turbulence values for onshore and offshore and considering different failure modes in the optimization. The impact of the upstream on the downstream turbines strongly depends on the ambient TI-value which is used. Offshore, the ambient TI is usually lower than Onshore because of the low surface roughness of the sea. Thus, TI-induced loads are generally lower than onshore, but differences between turbines are higher. To illustrate the influences of those differences on the planning, we present results for Onshore- and Offshore-scenarios where the ambient TI values strongly differ. Onshore, the 50 % Quantile of IEC class B is used (IEC, 2019a) and offshore the mean value of measurements from met mast Fino1 in the North Sea (Türk and Emeis, 2010). The ambient wind distribution from offshore is also used for the Onshore-scenario, to clearly see these effects. Due to this fact, the AEP for the Onshore-scenario is significantly higher than usual. This also has a strong effect on the economic evaluation with different cost assumptions for onshore and offshore taken from Stehly et al. (2024). Therefore, significantly different constant electricity

245

250



prices are selected in order to get comparable results on the NPV for all cases. All parameters for each the cases are summarized in Table 5.

**Table 5.** Overview of parameters for the use cases: Failure modes, Ambient TI and economic values

No.	Scenario	Failure mode	Ambient TI	CAPEX per MW	OPEX	Conversion rate	WACC	El. price
1	Onshore	Tower bm	IEC class B	1.968 Mio \$/MW	43 \$/MW/year	0.86 €/€.	6.5 %	6 ct/kWh
2	Offshore	Tower bm	Fino1	5.411 Mio \$/MW/year	135 \$/MW	0.86 €/€.	6.5 %	12 ct/kWh
3	Offshore	All three	Fino1	5.411 Mio \$/MW/year	135 \$/MW	0.86 €/€.	6.5 %	12 ct/kWh

In all cases, we assume that the wind farm is designed, so that the turbine with highest damage progression can operate for 25 years. In this case, a nominal operational  $\Delta^{P,nom}$  plan with all turbines operating at  $\Delta_{ij}^{P,nom} = 100\%$  of power at all times is used. Therefore, we first compute

$$D_{fm,i}(\Delta^{P,nom}, h^{eval}), \forall i \in \{1, \dots, N_T\}, \forall fm \in \mathcal{F}. \quad (11)$$

The lifetime of each turbine is computed under the assumption of a nominal lifetime of 25 years by using Eq. (7) with the finer binning distribution  $h^{eval}$ , i.e. calculating  $\tau_{fm,i}(\Delta^P; h^{eval})$  for each turbine and failure mode. The optimization problem described in Eq. (10) is solved using the coarser binning  $h^{opt}$  for all calculations. The evaluation is done with the finer binning afterwards.

The nominal lifetime of the tower, with no derating applied, is shown in Fig. 4 for the On- and Offshore cases. The tower lifetime of the turbine in the center is 25 years for both cases. Offshore, the turbine in the lower left corner could operate 4 years longer. In the Offshore case, differences among the turbines are significantly higher and lifetime of the turbine in the lower left corner is almost 20 years longer (43 years in total) compared to the turbine in the center. In total, all turbines' loads are significantly lower in the offshore case due to the lower ambient TI. But for this study, we are mainly interested in the relative differences between the turbines.

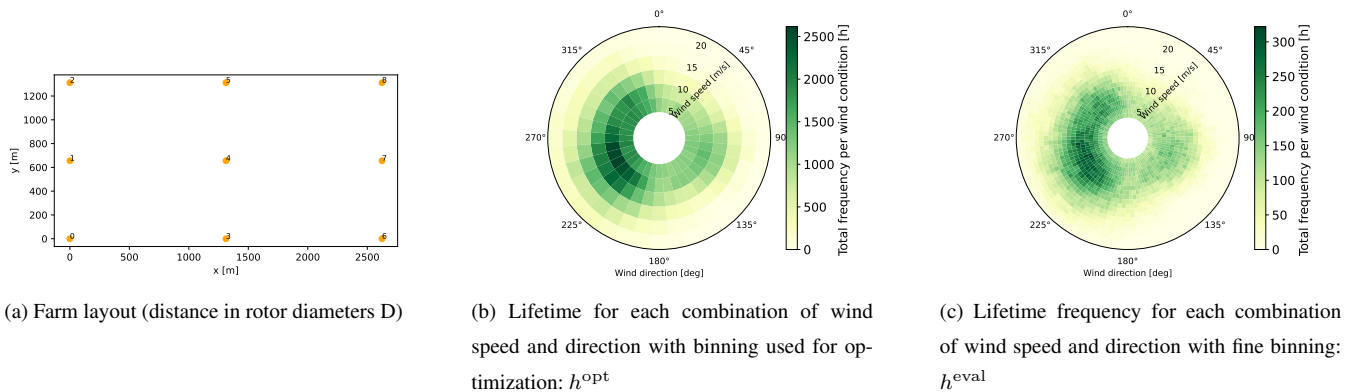


**Figure 3.** Wind farm layout and wind distribution with different binnings

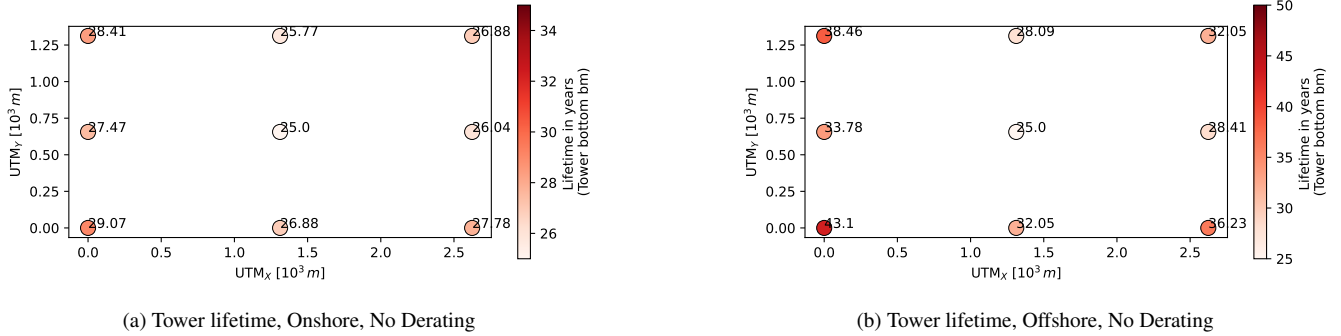


**Figure 4.** Nominal lifetime (no Derating) of the tower for On- and Offshore case (tower bm)

For all three use cases, we compare the optimal result from solving the full farm optimization problem (10) in a single run, with the iterative per-turbine approach. The energy production is always maximized over the original lifetime of 25 years under the constraint of different target lifetimes for the turbines. The target fatigue budget is given by the reciprocal value, i.e. by  $D_{\text{target}}^{\text{tower}} = \frac{25}{\tau_{\text{target}}^{\text{tower}}}$ . The AEP and the NPV with different target lifetimes are compared for both methods in all three cases. Subsequently, one of the results of each case is presented in more detail by showing the results for each turbine and the optimized derating plan. In the first two cases, the details are shown when the lifetime of all turbines is balanced. In the appendix, the course of energy production and NPV over the operating years (Sect. A) as well as an evaluation of different binning sizes is presented additionally (Sect. B).

#### 4.1 Case 1: Tower lifetime with onshore turbulence scenario

In this scenario, we solve the optimization problem for different target constraints for the selected failure mode of all turbines. The target fatigue budget is given by the reciprocal value, i.e. by  $D_{\text{target}}^{\text{tower}} = \frac{25}{\tau_{\text{target}}^{\text{tower}}}$ . We aim for target lifetimes  $\tau_{\text{target}}^{\text{tower}} \in \{27, 29, 30, 35\}$ , i.e. 2, 4, 5, and 10 years of extension. The turbine with the lowest lifetime is always assumed to determine the lifetime of the total wind farm and only full operational years are considered (see Sect. 2.4). For evaluation, we use the finest binning ( $h^{\text{eval}}$ ;  $\theta$ : 3 degrees, bin width for wind speed  $v$ : 1 m/s).

In Fig. 5, the AEP and the NPV are plotted over the lifetime of the farm as defined above. The curves for the two methods are almost identical for lifetimes up to 30 years and the difference in energy production and NPV is less than 0.2 %. The full farm optimization always yields a slightly higher value. The target lifetime of 35 years cannot be reached with both methods. While this is caused by differences from the fine binning and the binning used for optimization in the full farm optimization, not all constraints could be fulfilled in the per-turbine approach. The targeted lifetimes are reached at a slight energy loss between 1% and 4% up to a lifetime extension of 5 years (20% more lifetime). 10 years of lifetime extension (40 %) result in an energy loss of 20 %. In comparison to the energy production, the NPV considers interest rates and thus penalizes a loss in AEP in early operating years additionally. With low AEP losses, NWP can be increased by up to 10 % due to lifetime extensions between 2 and 5 years. An extension of 10 years reduces the AEP production and thus even leads to a reduction in NPV compared to the nominal cases. The highest NPV is reached after a lifetime of 29 years which is now discussed in more detail.

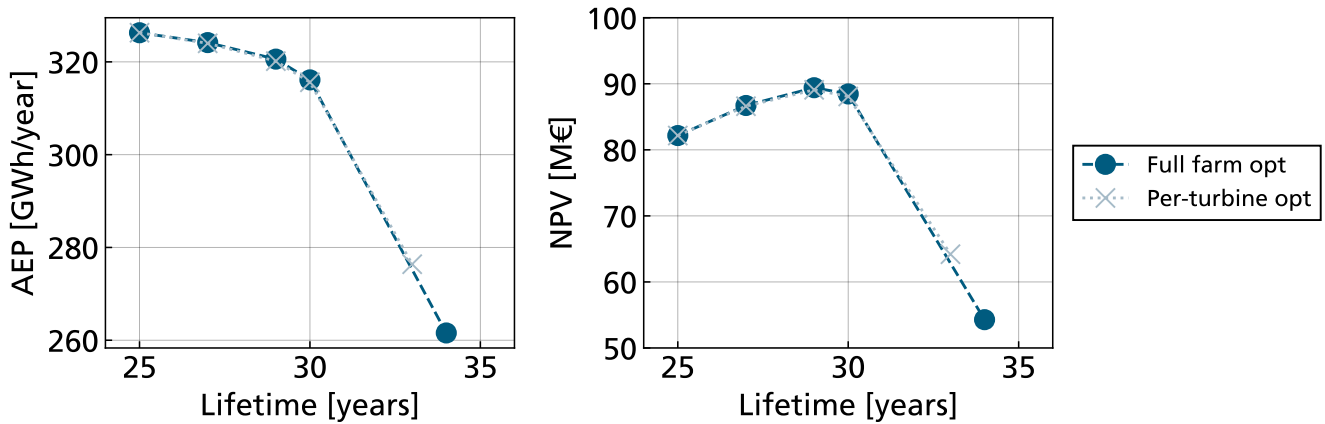


**Figure 5.** Case 1, Onshore scenario with different target values for tower lifetime: Comparison of AEP and NPV for the optimization approaches

With nominal operation, the turbine with the highest lifetime could operate for 25 years when considering the selected failure mode. With this target value, the lifetime of all turbines can be balanced at that value. Fig. 6 shows the tower lifetime and the AEP for each of the 9 turbines with both optimization approaches. With both approaches, the target lifetime of 29 years is slightly exceeded, and all turbines reach a value between 29 and 30 years.

295 The AEP is reduced strongest at the turbine in the center (index 4). When evaluating the relative difference in lifetime and AEP compared to the nominal case with no derating applied (Fig.7) two things can be observed. As seen in Fig. 5, the difference between the two optimization approaches is very low. The AEP with the full farm optimization is less than 1 % higher at turbine 4. In addition, the relative lifetime extension for all turbines is significantly higher than the loss in AEP. For turbine 4, 20 % more lifetime can be achieved at 5 % energy loss. When comparing the resulting operational plans in Fig. 8,

300 one can see similarities and differences in the results. A derating plan can be applied to best reduce damage for a turbine by itself. Derating is primarily applied when a turbine operates in the wake of others or at low wind speeds. In addition, upstream turbines reduce power in some cases when it is beneficial for turbines downstream. Due to the upstream derating, the amount and number of deratings can be reduced at downstream turbines. When comparing the results for the turbine in the center, the turbine can operate more often at full power while still meeting the required target damage. This is especially visible for

305 no-wake situations, e.g. between 15 and 65 or between 125 and 160 degrees. The differences in the operation plans are thus explainable because the optimizer can find a higher value for the farm energy and are still almost negligible for the overall AEP.

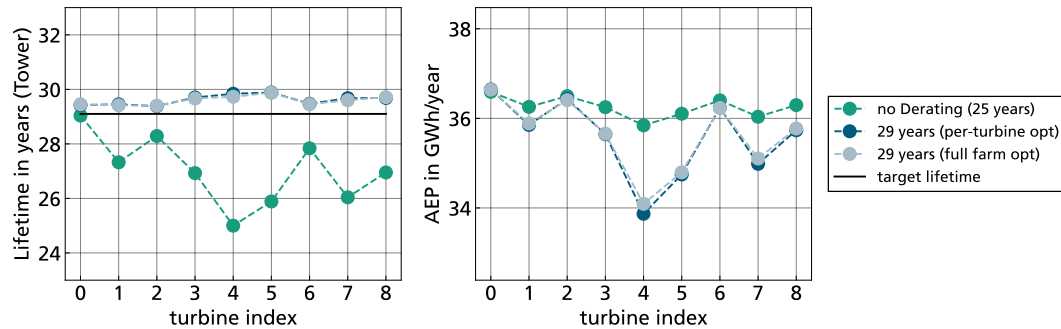


**Figure 6.** Case 1, Onshore-scenario balancing tower lifetime at 29 years: Absolute lifetime and AEP on each turbine for both optimization methods

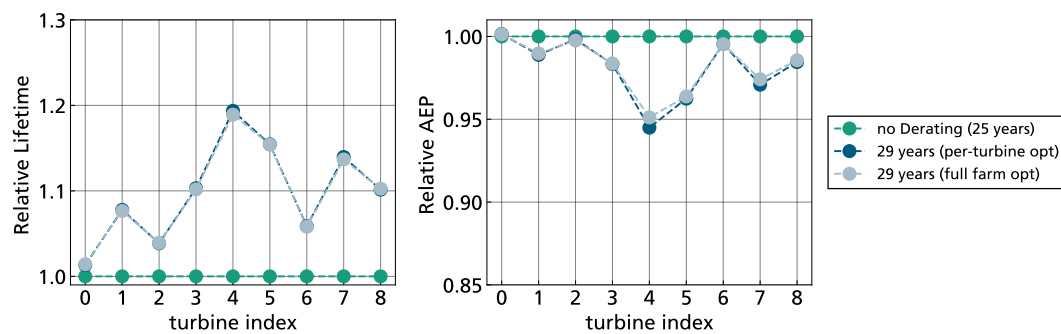


**Figure 7.** Case 1, Onshore-scenario balancing tower lifetime at 29 years: Relative values compare to nominal operation (no Derating) for lifetime and AEP on each turbine for both optimization methods

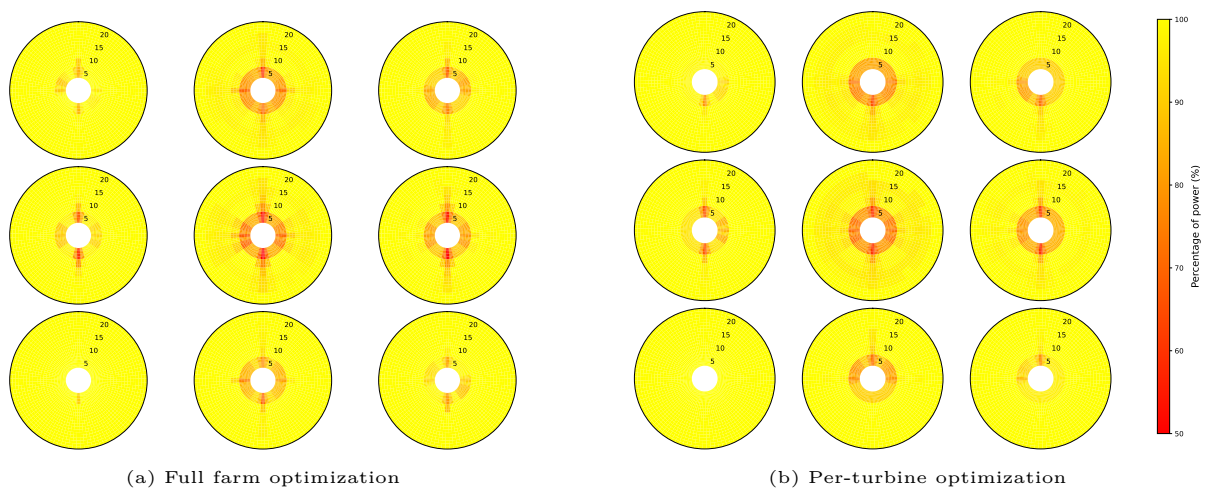


**Figure 8.** Case 1, Onshore-Scenario with tower as failure mode: Optimized operational plan from both optimization methods





#### 4.2 Case 2: Tower lifetime with offshore turbulence scenario

For this use case, we are also aiming for different target values for extending the lifetime of the wind farm (2, 5, 10 and 20 years), i.e.  $\tau_{\text{tower target}}^{\text{tower}} \in \{27, 29, 30, 35\}$ . The results for AEP and NPV are shown in Fig. 9 where, again, the main evaluation is done with the finest binning. In this scenario, aiming at a lifetime of 29 years for all turbines only requires a load reduction on three turbines (see Fig. 4b or green curve in Fig. 10). Therefore, the energy-loss of the complete farm is negligibly small (less than 0.1%) and a significantly higher NPV (41%) can be achieved when operating the farm 2 more years. A lifetime extension of 10 years yields the highest NPV under the given conditions. This also applies for both optimization methods, the full farm optimization and the per-turbine approach. When considering lifetimes below 30 years, the difference between both approaches remains minor because only few turbines are concerned with a small need for reducing damage. At 35 years, the AEP loss with the per-turbine approach is about 0.8 % lower resulting in an NPV difference of almost 5 % compared to the full farm optimization. When aiming at balancing the lifetime after 45 years of operation, the loss in NPV with the full farm optimization is so high, that the NPV is lower than after 35 years but still higher than after 25 years. With the per-turbine optimization, the target lifetime constraint cannot be fulfilled for some turbines and the lifetime is only 37 years with a higher loss in NPV and energy production.

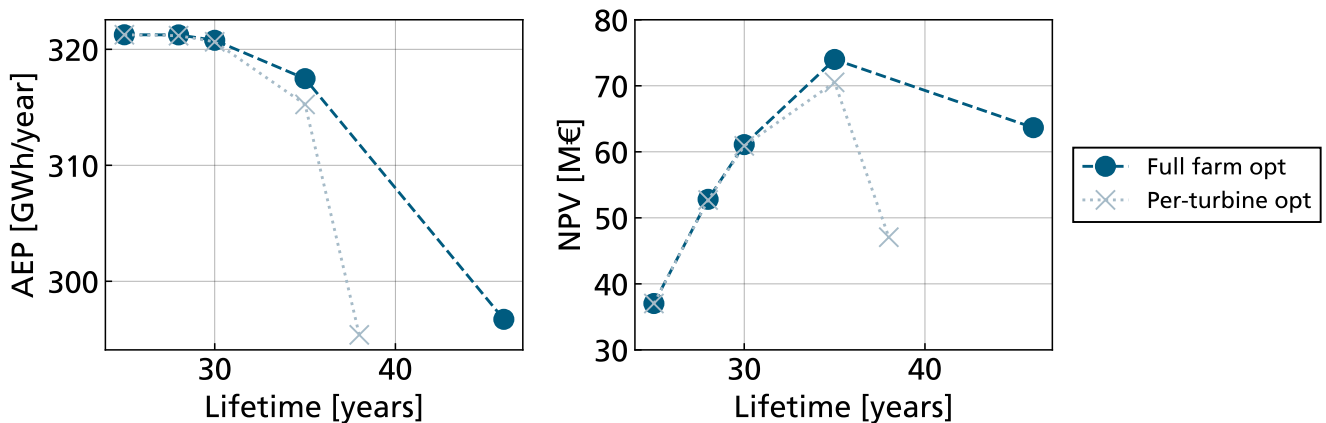


**Figure 9.** Case 2: Offshore scenario with different target values for tower lifetime: Comparison of AEP and NPV for the optimization approaches

This result is now discussed in more detail. In Fig. 10, it can be observed that the targeted lifetime cannot be reached by three out of the 9 turbines with the per-turbine optimization while the target is met with the full farm approach. When studying the AEP, it can be observed that the energy AEP of some turbines needs to be reduced significantly (index 0,1,2,6) to enable less derating at turbines 4 and 5, resulting in an overall higher AEP.

With the per-turbine approach, the three turbines not reaching the target lifetime are derated to their maximum level (Fig. 12). At most wind speeds, derating down to 50 % induces higher loads than a moderate derating to about 80 % which is selected by



the optimizer. With the full farm optimization, upstream turbines are derated to their maximum level in some wind directions (e.g. 90 degrees for the lowest row, 0 degrees for the upper row). Especially downstream turbines with a low distance (4D in horizontal direction) derate at all wind speeds for relevant wind directions to spare the turbines downstream. This way, the lifetime of the turbine with the lowest lifetime can be increased to the target value without it having to derate under all conditions. Due to the lower ambient TI, the influence of derating on the wake-induced turbulence is higher and more effective for the load reduction on downstream turbines. With the relative values shown in Fig. 11, it can again be seen that the relative lifetime extension is significantly higher than the loss in AEP for all turbines, e.g almost 80 % more lifetime for turbine 4 in the center at only 10% AEP reduction.

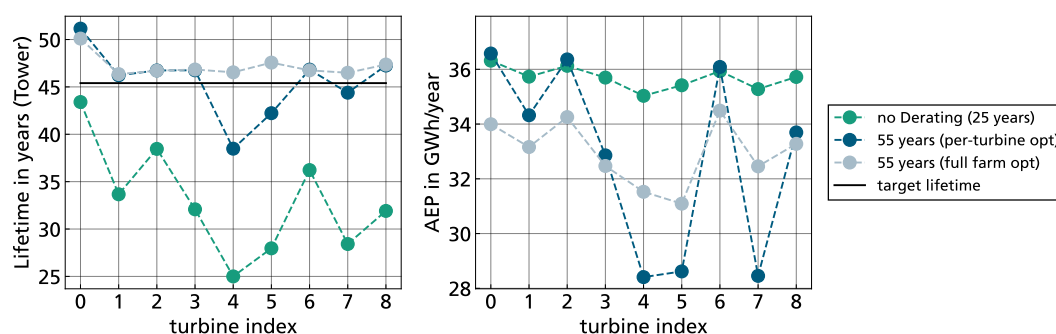


**Figure 10.** Case 2, Offshore scenario balancing tower lifetime at 45 years: Absolute lifetime and AEP on each turbine for both optimization methods

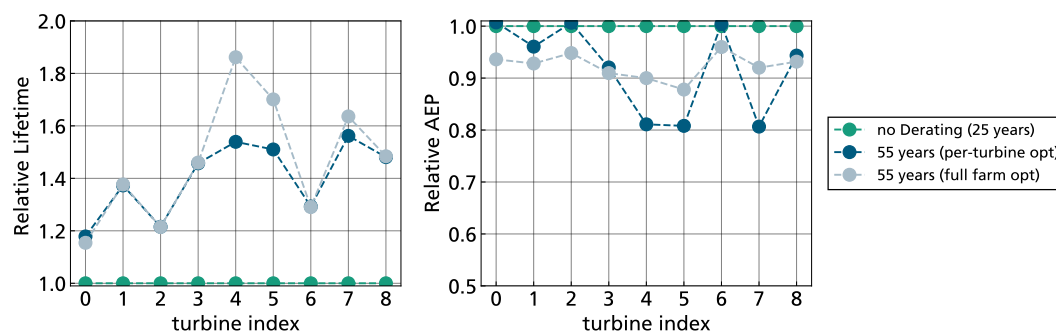


**Figure 11.** Case 2, Offshore-scenario balancing tower lifetime at 45 years: Relative values compare to nominal operation (no Derating) for lifetime and AEP on each turbine for both optimization methods

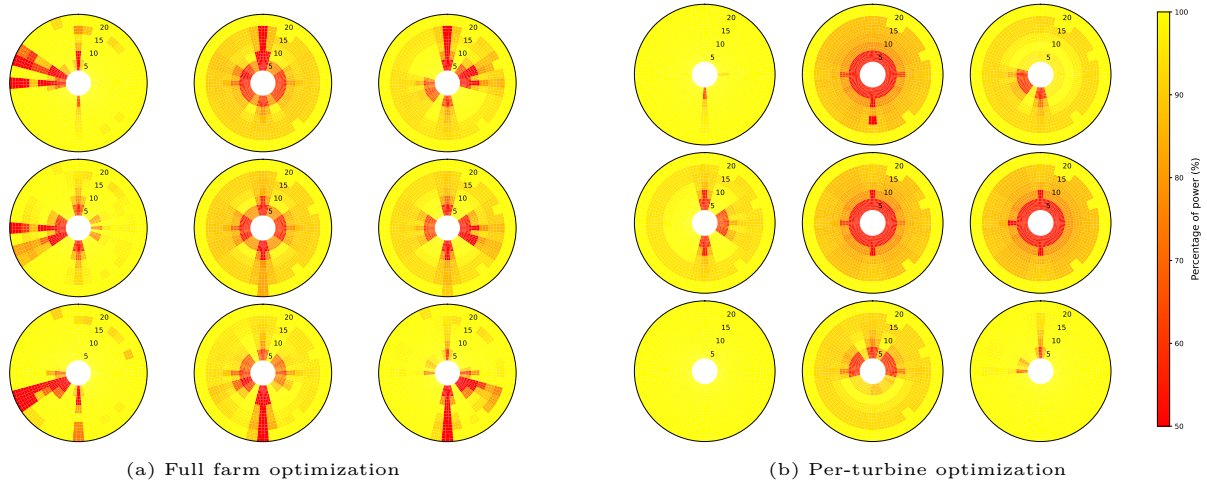


**Figure 12.** Case 2, Offshore-scenario balancing tower lifetime at 45 years: Optimized operational plans from both optimization methods

### 4.3 Case 3: Lifetime extension on all selected failure modes in Offshore-scenario

In the third scenario, we impose two lifetime targets across all turbines and all failure modes: 27 and 30 years, i.e. 2 and 5 years of extension ( $\tau_{\text{target}}^{\text{fm}} \in \{27, 30\}, \forall i, \forall \text{fm}$ , resulting in 27 constraints in total). All three considered failure modes show a different behavior dependent on the influencing parameters wind speed, turbulence intensity and derating factor. While the tower bending moment and the flapwise blade root bending moments are strongly influenced by the turbulence intensity, the edgewise moment is mainly driven by the rotational speed due to gravitational loads. Thus, the wake-induced differences in lifetime between turbines are very low. Due to the low influence of TI, the edgewise bending moment is the dominant failure mode, when all failure modes are considered in the computation of the total farm lifetime (using Eq. (8) for the computation of the total farm lifetime). For a better understanding of the result, we first discuss the lifetime extension to 27 years in detail.

340 The nominal lifetimes without derating for all three failure modes can be seen in the green curves in Fig. 13 and Fig. 14.

For the failure mode represented by the edgewise bending moment, the lifetime of all turbines is approximately 25 years and can be extended to almost 28 years (about 10 %) on all turbines at an average AEP loss of about 6 % (see Fig. 15). The lifetime on all turbines and failure modes is higher than 28 years in this case, i.e. all constraints are fulfilled. The comparably high energy loss results from the dependency on the edgewise loads on the rotational speed. For this reason, it is difficult to

350 improve the relationship between induced damage and energy production. The results for the full farm and the per-turbine optimization are almost identical, with minimally higher AEP for the full farm approach. The lifetime of the other two failure modes is strongly increased for all turbines and above the target (see Fig. 14).

When studying the optimized operational plan for this optimization run, two patterns can be observed (Fig. 16): A derating to 90 or 80% is applied on all turbines for almost all wind speeds and directions below 15 m/s with both optimization approaches.

355 At this level of derating, the rotational speed is reduced significantly and thus leads to the most effective reduction of damage.



The resulting plan thus differs from the previous optimized plans in the other two use cases significantly. With the full farm approach, upstream turbines also reduce their power in full wake situations in the partial load region between 4 and 7 m/s down to 50 or 60 %. Despite these differences in the operational plan, the resulting AEP is almost the same. The results are determined by the underlying relationship of wind, wake effects and influence of the controller and the optimizer is able to find the best possible relationship under the given constraints.

Fig. 17 shows the AEP and NPV for the two target lifetimes. The lower AEP is too significant for the initial investment and level of interest rate so that the final value of NPV is lower by 60% after 27 years of operation. By aiming at 29 years of operation, the NPV is even below 0.

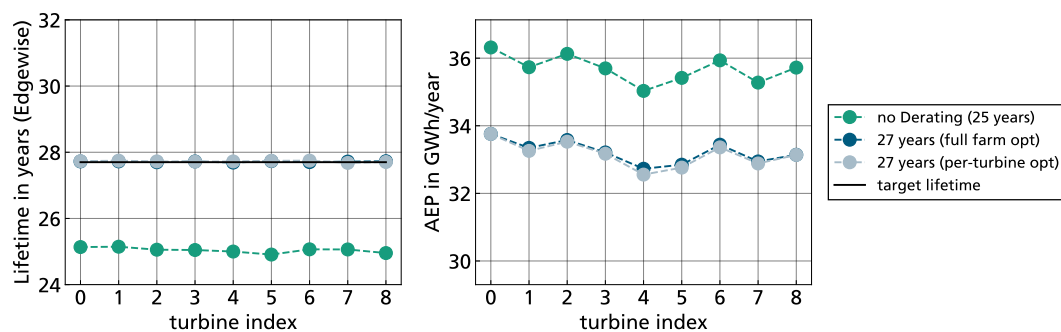


**Figure 13.** Case 3, Offshore-scenario with all failure modes: Absolute lifetime and AEP on each turbine for both optimization methods

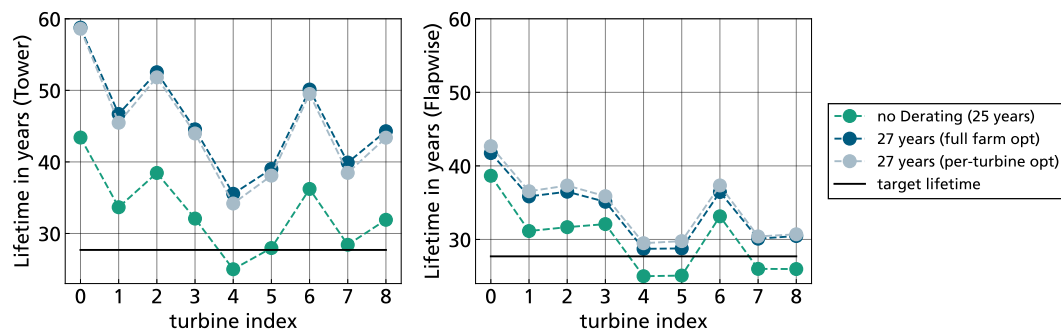


**Figure 14.** Case 3, Offshore-scenario with all failure modes: Absolute for lifetime for flapwise blade bm and tower bm on each turbine for both optimization methods

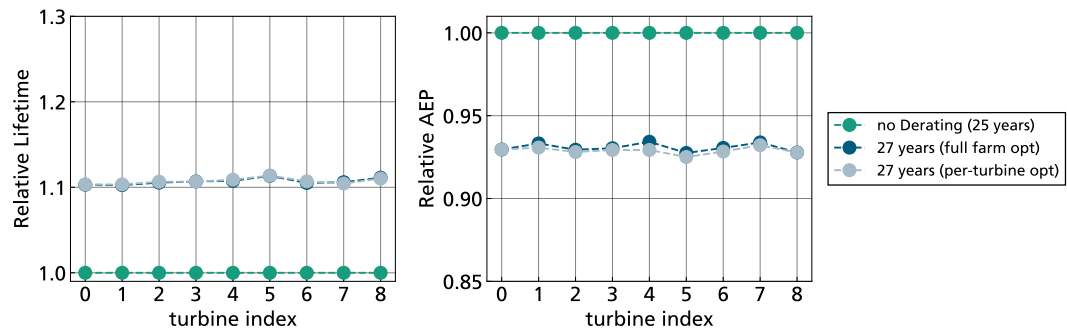


**Figure 15.** Case 3, Offshore-scenario with all failure modes: Relative values compare to nominal operation (no Derating) for lifetime and AEP on each turbine for both optimization methods

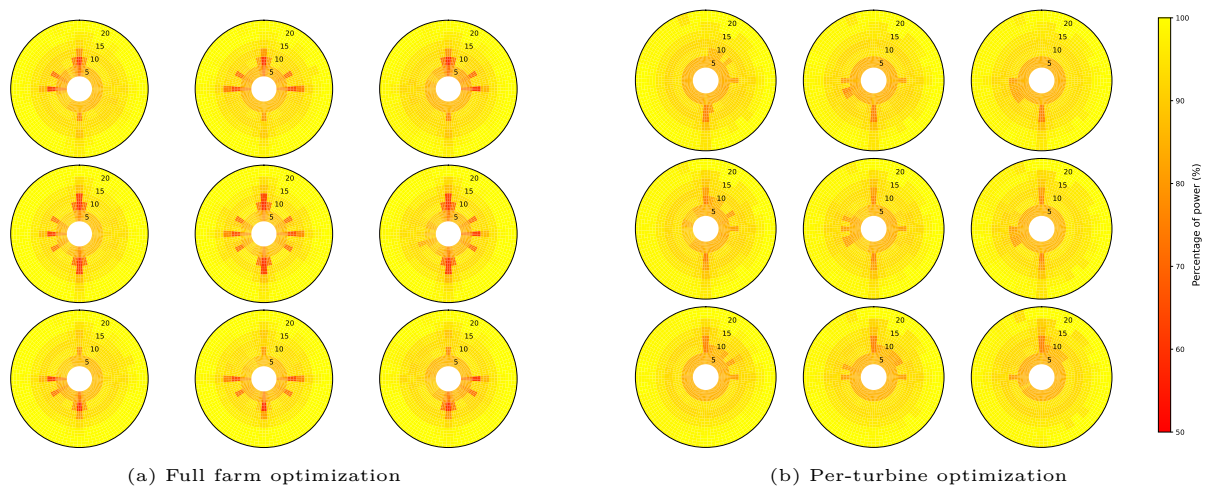


**Figure 16.** Case 3, Offshore-scenario with all failure modes: Optimized operational plans from both optimization methods

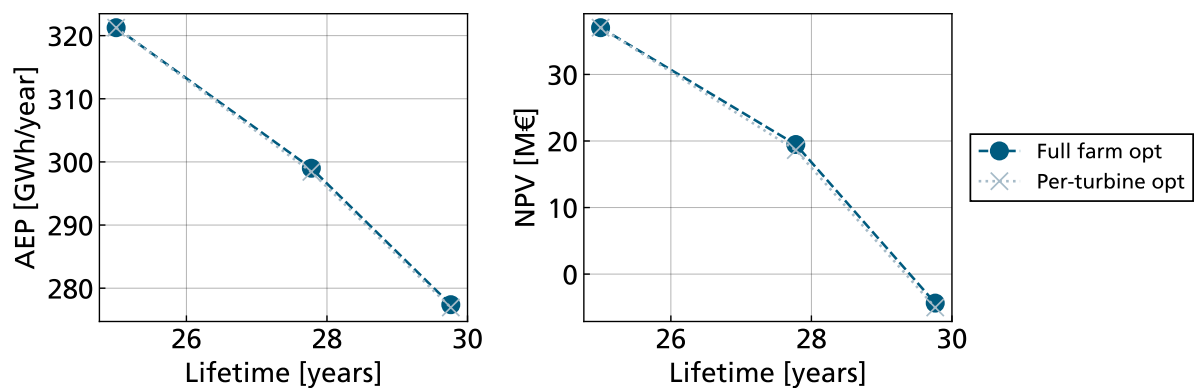


**Figure 17.** Case 3, Evaluation of results: Offshore-scenario, balancing tower lifetime



## 5 Discussion

365 The application of VIOLA to the example wind farm indicates that a condition-based operational planning can redistribute damage away from operating situations with an unfavorable relation between energy and damage, while preserving energy yield where the trade-off is more advantageous.

In all of the studied cases, the optimization systematically reduces the fatigue damage by the amount of derating, so that the overall energy production is maximized and improves the damage-energy relationship of each individual turbine and the full wind farm. When only considering the tower bm as a failure mode, fatigue damage can be strongly reduced under some conditions so that the loss in energy production is significantly lower in total. A consistent observation is that derating still yields its largest benefit on the derated turbine itself. The consideration of derating of upstream turbines has an impact on the optimal achievable energy production of the farm which can only be captured by the full farm optimization approach. This impact depends on the scenario and on the targeted lifetime extension for the different failure modes. In most of the studied cases, the difference in AEP between the full farm and the per-turbine optimization was low. Despite that the resulting operational plans differ and the full farm approach uses derating of upstream turbines to yield the best overall result, the AEP gain compared to the per-turbine approaches is less than 1 % in almost every case. The benefit of the full farm approach mainly applies when many of the turbines require a significant derating and under offshore turbulence conditions.

When multiple failure modes are considered, turbulence-driven modes (e.g., tower bottom bending, blade flapwise root loads) respond well to the wake-aware derating, whereas gravity/rotational-speed-driven modes (blade edgewise) require high reductions in rotational speed and therefore incur higher energy losses. By comparing Onshore- and Offshore-scenarios for the ambient turbulence intensity, the influence of this parameter on the wake and subsequently on the fatigue lifetime is shown exemplarily. With a higher ambient turbulence, the flow behind the turbine adapts more quickly to the surrounding conditions and thus reduces variability of loads between the turbines. With a lower ambient TI, the reduction of the thrust of upstream turbines more effectively reduces the TI downstream.

When interpreting results for farm lifetime, lifetime energy, and NPV, note that the evaluation is intentionally simple and supports first-order comparisons. We show that higher NPV can be achieved by modestly extending lifetime at the expense of a small reduction in AEP. The assumption on lifetime and decommissioning based on a deterministic and relative consideration of lifetime fatigue damage is strong and should not be applied directly to real projects. The basis for the fatigue damage calculation in the optimization process is the same as for design calculations and can thus be integrated into the planning process of wind farm operation.

In addition to the uncertainties in the long-term evaluation of the economic benefits, the results also depend on the underlying models which are used on several levels, i.e. the configuration of the turbine controller, the surrogate models for the fatigue damage calculation, and the wake models. Controller-specific choices influence how loads and the wake respond to derating. The surrogate approach based on DELs and linear damage accumulation is tractable and standard for design-oriented assessments, but it does not capture sequence effects or material nonlinearities that can be relevant for composites. Many of these points have been discussed in detail in (Requate and Meyer, 2023) because the modeling uncertainties also apply when





a single turbine is considered. In the wind farm context, the wake modelling approach also influences results. Firstly, dynamic effects cannot be represented with steady-state models. Secondly, the parameters of the steady-state model influence the effect of the turbines on the wake.

Under the given model assumptions and parameters, the optimizer attempts to find the best possible solution. Essentially, the problems for a per-turbine approach and for the wind farm both nonconvex NLPs, making them suitable for nonlinear gradient-based optimizers. On the one hand, we cannot guarantee that a global or even local optimum of the problem is found because of the nonconvexity and unfulfilled requirements in the underlying functions. On the other hand, the shape of the resulting operational plans as well as the consistent results in all of the studied cases assure that an optimal or close-to-optimal solution is found in all cases.

Nevertheless, the gradient-based solution process suffers from an objective function which can be very flat close to the optimal solution. This effect is caused by the frequency distribution, which has very low values under some conditions, especially at higher wind speeds in some wind directions. This effect affects both optimization approaches but also scales with the number of turbines in the full farm approach.

Overall, the iterative per-turbine optimization scales easily and is attractive to use when the coupling between turbines is weak or when moderate lifetime extensions on some turbines are targeted. Pragmatic workflows which combine partial solutions on small subsets of larger farms, combined with the iterative process, could be tested. In addition, heuristic solutions which incorporate additional knowledge on the problem behavior could be integrated and potentially combined with nonlinear optimization. The optimization problem can still increase strongly in size with larger wind farms; a finer binning of conditions, more conditions, or other control setpoints (like yaw misalignment) should be considered. On the one hand, this can be done by further fine-tuning the setup of the optimization problem, e.g. by implementing analytical gradients automatically or through decomposition of the problem.

## 6 Conclusion and Outlook

We present a condition-based planning method that redistributes fatigue damage over turbine lifetime by combining surrogate models with a long-term optimization. We compare two optimization approaches and show, across use cases, how optimized operational plans can extend lifetime for some or all turbines in a wind farm and increase revenue through longer operation. The method identifies operational plans that reduce damage in wake-affected, high-turbulence conditions while retaining energy in more favorable situations, resulting in a more efficient relationship between energy production and fatigue damage for each turbine. We show that an individual per-turbine optimization process is almost as effective as the approach for optimizing the full wind farm including all wake-interaction effects for the dedicated problem. The optimization process was applied under different turbulence conditions (onshore- and offshore) and under consideration of different failure modes. Especially onshore, the wake-interaction between turbines is lower and upstream derating only has a small influence on downstream TI and subsequent damage.





430 The benefits of the approach for optimized operational planning are quantified for the 9-turbine example farm: Onshore, extending tower lifetime by 2–5 years lowers AEP by only 1–4% and raises NPV by up to 10%. For the turbine with the highest required reduction of loads, lifetime is extended by 20 % at an energy loss of only 5 %. Offshore, extending tower lifetime of the highest loaded turbines by up to 5 years only requires the derating of a few turbines. This is possible at very low AEP losses of less than 0.2 % resulting in high NPV raises by more than 50 %. For larger lifetime extensions, a significant  
435 reduction in AEP is required (up to 20 %) to extend the lifetime by 80 % so that NPV is still higher than in the nominal case with no derating applied. When blade edgewise loads are included, reaching 28 years requires 6 % AEP reduction and sharply reduces NPV (60 %), reflecting the strong rotational-speed sensitivity.

In total, we can find an optimal relation of consumed fatigue life and energy production for a given target and thus contribute to a more efficient way of operating wind farms and each individual turbine within the farm. With the modular optimization  
440 framework, the groundwork for further developments is made. The iterative approach represents a scalable solution for large wind farms. It can be integrated into a pragmatic workflow for optimized wind farm planning. The full farm approach can initially be used as a comparative solution for parts of the farm for validation purposes, or it can be scaled to large farms using improved methods and longer computing times.

A key challenge and barrier for practical implementation is quantifying how reductions in predicted fatigue loads translate  
445 into changes in failure probability and mean time to failure under real operating conditions. This issue can partially be addressed by improving the underlying models and assessing uncertainties and sensitivities. Nevertheless, the process is in-line with current standard-methods for design load calculations of wind turbines according to IEC (IEC, 2019b). However, the advantage of energy loss must be clearly demonstrated to an operator in order to make such a strategy applicable. To further prove the benefits of applying such more individual operational strategies on the turbines, an extensive stochastic analysis considering  
450 uncertainties and different end-of-life scenarios would be required. Any long-term plan depends on assumptions about the wind climate and the economic development. Frequency distributions derived from historical data are practical and commonly used, but they do not fully capture seasonal and interannual variability or longer-term shifts.

In addition, the economic evaluation is sensitive to price trajectories, discount rates, and maintenance cost assumptions. For this reason, deterministic results should be interpreted alongside scenario analyses or sensitivities. Periodic re-planning with  
455 updated site data and asset condition, combined with simple Monte Carlo sampling over wind roses and economic parameters, can provide a more robust view of risk and value.

Some of the advantages of the operational planning cannot be estimated by the simple economic evaluation as done within this work. In addition to stochastic analysis to address uncertainties, the benefits of a more coordinated end-of-life among the turbines need to be investigated. Furthermore, such strategies can explicitly be used to reduce the design fatigue budget or to  
460 adapt a turbine to a site with more severe operational conditions than assumed during the design process.

A further step for practical usage is the integration of external influences beyond the environmental conditions. Especially, the integration of electricity prices into the planning process will be relevant for future wind farms operating in a flexible market. In addition, it could also be investigated how the energy reserve can be used for the balancing market. The evaluations in this study also assumed that the optimized operational plan would be applied consistently throughout the lifetime. It would



465 also be possible to change the plan after a few years of operation, for example, if an extension of the lifetime is desired or if an annually variable plan is to be optimized, as in (Requate et al., 2024).

Regarding the implementation in a wind farm controller, the optimized plan is delivered as a look-up table of derating setpoints per turbine and bin of wind direction and speed. This is compatible with most turbines, since derating is standard for grid power tracking. In operation, the interval width for binning should be aligned with sensing of the environmental conditions  
470 and filtered to avoid frequent switching. Wind direction and speed estimates from SCADA or lidar can be used. As the plan is applied, safeguards must ensure compliance with certification and address setpoint-specific risks (e.g., negative damping offshore). Over time, the planning can be refreshed with updated site data, asset condition and economic assumptions, and extended with targeted uprating or additional control channels (like wake steering) to improve the lifetime–energy trade-off.



## List of symbols

475 *Code and data availability.* Codes and data were created for each step of the published method. The Python-tool VIOLA is developed specifically for an in-house workflow and only partially documented. Thus, there is no single self-contained program of which sharing would provide value for others yet. The code can be shared upon personal request to the authors. The dataset of short-term DELs, used to create the surrogate models, can be found at <https://doi.org/10.5281/zenodo.8385296>. For inquiries about data or code, please contact the authors.

*Author contributions.* NR developed the concept for the study and the research methods. NR developed the code and produced the results  
480 under supervision and with valuable input from LV. RH reviewed the draft version and gave valuable feedback on the draft, the concept and the results. NR reviewed and edited the draft version.

*Competing interests.* The authors declare that they have no conflict of interest.

*Acknowledgements.* The research was carried out by Fraunhofer IWES under the framework of the FlexiWind- project (FKZ: 03EE3071A) funded by the Bundesministerium für Wirtschaft und Energie (BMBE).

## 485 **Appendix A: Net present value calculations**

To illustrate how the interest rate translates energy production into NPC, Fig. A1 and Fig. A2 show the course of the total energy production and the NPV over the operating years for all use cases with the full farm optimization approach. By taking interest into account, the linear growth of energy production translates to a nonlinear course of NPV over the years. While energy production is higher than nominal operation for all the optimized results NPV can decrease when the AEP is too high.

## 490 **Appendix B: Comparison of binning sizes**

To study the sensitivity of the results on the selected binning size of the ambient conditions, the evaluations for different binnings are compared for all the studied cases with the full farm optimization approach (Fig. B1, Fig. B2 and Fig. B3). When comparing all results, the relative course of the curves is very similar for both AEP and NPV. With the broadest binning (dotted curve), a strong deviation can be observed even for the nominal lifetime. In this case, the area for the wake effects is too broad  
495 and neglects some effects which seem sufficiently captured with a bin width of  $10^\circ$ . In addition, the derating setpoints are applied to a broader area and thus reduce efficiency. With the selected bin sizes from Table 4, a good compromise seems to be chosen for finding an optimized plan under the given assumptions.

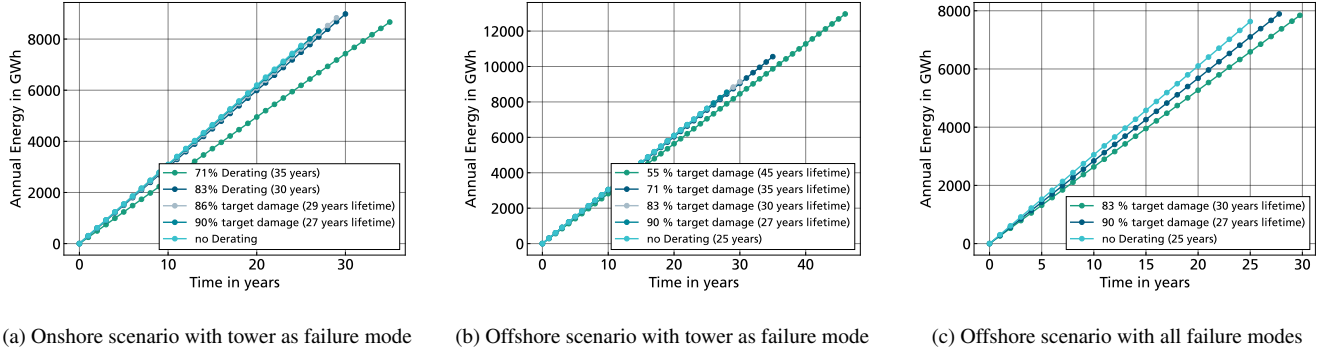


**Figure A1.** Total energy production over operating years of the wind farm in different scenarios using the full farm optimization

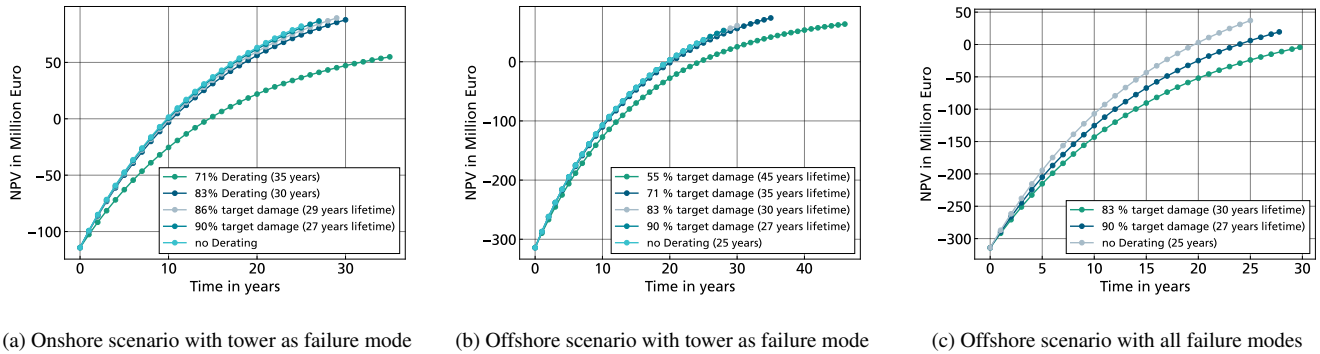


**Figure A2.** NPV over operating years of the wind farm in different scenarios using the full farm optimization

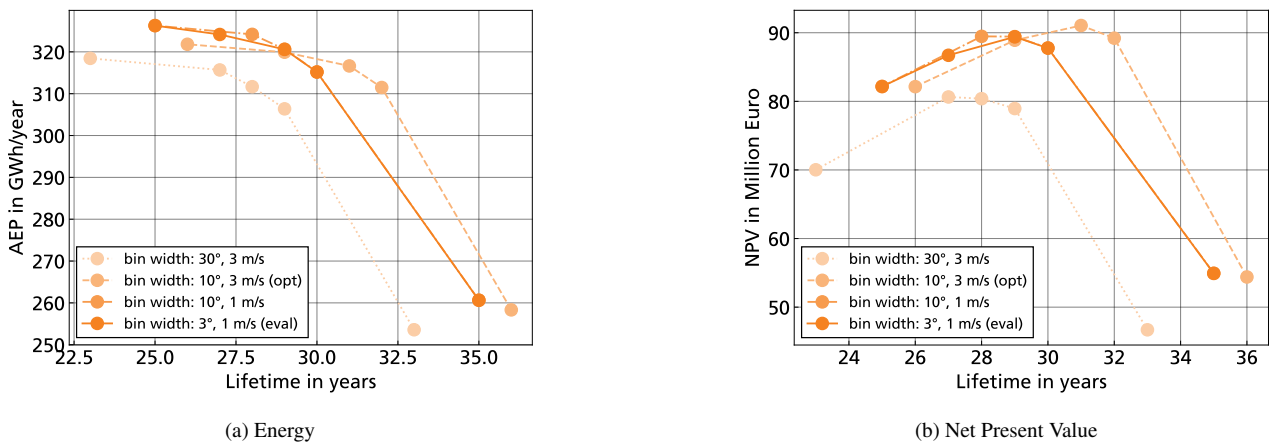
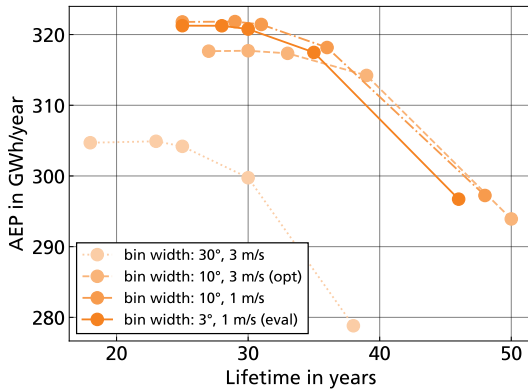
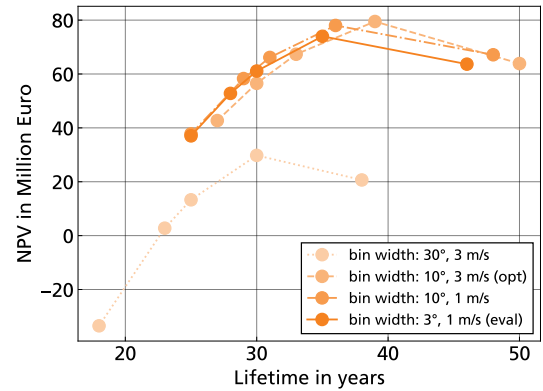


**Figure B1.** Case 1, Onshore scenario with tower as failure mode: Comparison of binning sizes of AEP and NPV

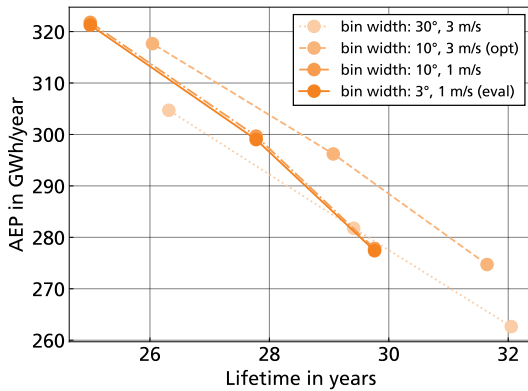


(a) Energy

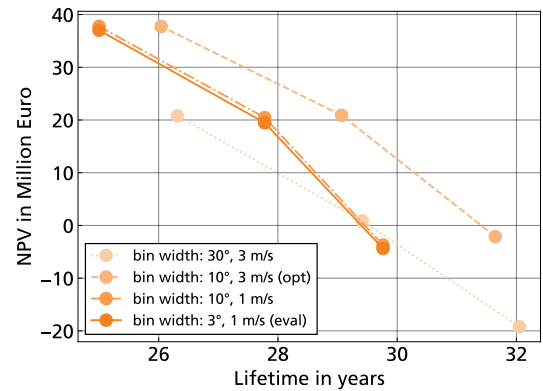


(b) Net Present Value

**Figure B2.** Case 2, Offshore scenario with tower as failure mode: Comparison of binning sizes of AEP and NPV



(a) Energy



(b) Net Present Value

**Figure B3.** Case 3, Offshore scenario with all failure modes: Comparison of binning sizes of AEP and NPV

## References

- Astrain Juangarcia, D., Eguinoa, I., and Knudsen, T.: Derating a single wind farm turbine for reducing its wake and fatigue, *Journal of Physics: Conference Series*, 1037, 032 039, <https://doi.org/10.1088/1742-6596/1037/3/032039>, 2018.
- Bastankhah, M. and Porté-Agel, F.: Experimental and theoretical study of wind turbine wakes in yawed conditions, *Journal of Fluid Mechanics*, 806, 506–541, <https://doi.org/10.1017/jfm.2016.595>, 2016.
- BDEW: Koordinierter Weiterbetrieb von Offshore-Windparks kann Kosteneffizienz und Stromerträge erhöhen, <https://www.bdew.de/presse/koordinierter-weiterbetrieb-von-offshore-windparks-kann-kosteneffizienz-und-stromertraege-erhoehen/>, 2025.
- Eguinoa, I., Göçmen, T., Garcia-Rosa, P. B., Das, K., Petrović, V., Kölle, K., Manjock, A., Koivisto, M. J., and Smailes, M.: Wind farm flow control oriented to electricity markets and grid integration: Initial perspective analysis, *Advanced Control for Applications*, 3, <https://doi.org/10.1002/adc2.80>, 2021.



- EMD International: WindPro 4.2 User Manual: 8c: Load Curtailment Optimization, [https://help.emd.dk/knowledgebase/content/windPRO4.2/c8c-UK\\_windPRO4.2-Load\\_Curtailment\\_Optimization.pdf](https://help.emd.dk/knowledgebase/content/windPRO4.2/c8c-UK_windPRO4.2-Load_Curtailment_Optimization.pdf), 2025.
- 510 Gharbia, I. B., Khvoenkova, N., Tona, P., Guillemin, F., Dupoirson, M., Quenedey, E., and Cousin, A.: A bin-wise approach to wake steering optimization under fatigue load constraints, *Journal of Physics: Conference Series*, 3025, 012 017, <https://doi.org/10.1088/1742-6596/3025/1/012017>, 2025.
- Gonzalez Silva, J., Ferrari, R., and van Wingerden, J.-W.: Wind farm control for wake-loss compensation, thrust balancing and load-limiting of turbines, *Renewable Energy*, 203, 421–433, <https://doi.org/10.1016/j.renene.2022.11.113>, 2023.
- 515 Guilloiré, A., Campagnolo, F., and Bottasso, C. L.: A control-oriented load surrogate model based on sector-averaged inflow quantities: capturing damage for unwaked, waked, wake-steering and curtailed wind turbines, *Journal of Physics: Conference Series*, 2767, 032 019, <https://doi.org/10.1088/1742-6596/2767/3/032019>, 2024.
- Hersbach, H., Bell, B., Berrisford, P., Biavati, G., Horányi, A., Muñoz Sabater, J., Nicolas, J., Peubey, C., Radu, R., Rozum, I., Schepers, D., Simmons, A., Soci, C., Dee, D., and Thépaut, J.-N.: ERA5 hourly data on single levels from 1959 to present, 520 <https://doi.org/10.24381/cds.adbb2d47>, 2018.
- Houck, D. R.: Review of wake management techniques for wind turbines, *Wind Energy*, 25, 195–220, <https://doi.org/10.1002/we.2668>, 2022.
- IEC: Wind energy generation systems – Part 3-1: Design requirements for fixed offshore wind turbines, 2019a.
- IEC: Wind Turbines - Part 1: Design Requirements, 2019b.
- International, E.: Lifetime Optimisation: Ensure wind turbine lifetime with windPRO optimisation, <https://www.emd-international.com/lifetime-optimisation>, 2025.
- 525 Jensen, T. N., Knudsen, T., and Bak, T.: Fatigue minimising power reference control of a de-rated wind farm, *Journal of Physics: Conference Series*, 753, 052 022, <https://doi.org/10.1088/1742-6596/753/5/052022>, 2016.
- Kölle, K., Göçmen, T., Eguinoa, I., Alcayaga Román, L. A., Aparicio-Sanchez, M., Feng, J., Meyers, J., Pettas, V., and Sood, I.: FarmConnors market showcase results: wind farm flow control considering electricity prices, *Wind Energy Science*, 7, 2181–2200, 530 <https://doi.org/10.5194/wes-7-2181-2022>, 2022.
- Liew, J., Riva, R., Friis-Møller, M., and Göçmen, T.: Wind Farm Control Optimisation Under Load Constraints Via Surrogate Modelling, *Journal of Physics: Conference Series*, 2767, 092 039, <https://doi.org/10.1088/1742-6596/2767/9/092039>, 2024.
- Meng, F., Hou Lio, A. W., and Liew, J.: The effect of minimum thrust coefficient control strategy on power output and loads of a wind farm, *Journal of Physics: Conference Series*, 1452, 012 009, <https://doi.org/10.1088/1742-6596/1452/1/012009>, 2020.
- 535 Meyer, T. and Requate, N.: Advanced concepts for control of wind turbine and wind farm systems, in: *Wind Turbine System Design. Volume 2: Electrical systems, grid integration, control and monitoring*, edited by Wenske, J., pp. 411–441, Institution of Engineering and Technology, [https://doi.org/10.1049/PBPO142G\\_ch9](https://doi.org/10.1049/PBPO142G_ch9), 2023.
- Meyers, J., Bottasso, C., Dykes, K., Fleming, P., Gebraad, P., Giebel, G., Göçmen, T., and van Wingerden, J.-W.: Wind farm flow control: prospects and challenges, *Wind Energy Science*, 7, 2271–2306, <https://doi.org/10.5194/wes-7-2271-2022>, 2022.
- 540 Nash, R., Nouri, R., and Vassel-Be-Hagh, A.: Wind turbine wake control strategies: A review and concept proposal, *Energy Conversion and Management*, 245, 114 581, <https://doi.org/10.1016/j.enconman.2021.114581>, 2021.
- Pacheco, J., Berezyak, M., Martins, J., Teixeira, N., Pereira, C., Figueiredo, R., and Oliveira, C.: Push power where you can and prevent damage where you need, *Journal of Physics: Conference Series*, 3025, 012 015, <https://doi.org/10.1088/1742-6596/3025/1/012015>, 2025.
- Pettas, V. and Cheng, P. W.: Surrogate Modeling and Aeroelastic Analysis of a Wind Turbine with Down-Regulation, Power Boosting, and 545 IBC Capabilities, *Energies*, 17, 1284, <https://doi.org/10.3390/en17061284>, 2024.



Requate, N. and Meyer, T.: Optimal Operational Planning of Wind Turbine Fatigue Progression Under Stochastic Wind Uncertainty, in: Proceeding of the 33rd European Safety and Reliability Conference, edited by Brito, M. P., Aven, T., Baraldi, P., Čepin, M., and Zio, E., pp. 1321–1328, Research Publishing Services, Singapore, [https://doi.org/10.3850/978-981-18-8071-1\\_P725-cd](https://doi.org/10.3850/978-981-18-8071-1_P725-cd), 2023.

550 Requate, N., Meyer, T., and Hofmann, R.: From wind conditions to operational strategy: Optimal planning of wind turbine damage progression over its lifetime, *Wind Energ. Sci. Discuss.* [preprint], <https://doi.org/10.5194/wes-2022-99>, 2022.

Requate, N., Meyer, T., and Hofmann, R.: Maximizing value through optimized annual selection of Pareto-optimal wind turbine operating strategies, *Journal of Physics: Conference Series*, 2767, 032 045, <https://doi.org/10.1088/1742-6596/2767/3/032045>, 2024.

555 Robbelein, K., Daems, P. J., Verstraeten, T., Noppe, N., Weijtjens, W., Helsen, J., and Devriendt, C.: Effect of curtailment scenarios on the loads and lifetime of offshore wind turbine generator support structures, *Journal of Physics: Conference Series*, 2507, 012 013, <https://doi.org/10.1088/1742-6596/2507/1/012013>, 2023.

Schmidt, J.: FOXES (Farm Optimization and eXtended yield Evaluation Software ), <https://fraunhoferiwes.github.io/foxes.docs/index.html>, 2022.

Stehly, T., Duffy, P., and Hernando, D. M.: Cost of Wind Energy Review: 2024 Edition, <https://docs.nrel.gov/docs/fy25osti/91775.pdf>, 2024.

560 Stock, A., Cole, M., Leithead, W., and Amos, L.: Distributed Control of Wind Farm Power Set Points to Minimise Fatigue Loads, in: 2020 American Control Conference (ACC), pp. 4843–4848, IEEE, <https://doi.org/10.23919/ACC45564.2020.9147732>, 2020.

Türk, M. and Emeis, S.: The dependence of offshore turbulence intensity on wind speed, *Journal of Wind Engineering and Industrial Aerodynamics*, 98, 466–471, <https://doi.org/10.1016/j.jweia.2010.02.005>, 2010.

Wachter, A. and Laird, C.: Ipopt, <https://coin-or.github.io/Ipopt/index.html>, 2022.

565 Ziegler, L., Schulze, A., and Henning, M.: Optimization of curtailment intervals of wind turbines through assessment of measured loads during start-up and shutdown events, *Journal of Physics: Conference Series*, 2767, 032 006, <https://doi.org/10.1088/1742-6596/2767/3/032006>, 2024.





Symbol	Meaning
$x^{\text{amb}} \in \mathbb{R}^W$	Ambient input vector (e.g., direction, speed, turbulence).
$W \in \mathbb{N}$	Number of selected ambient variables.
$X^{\text{amb}} \in \mathbb{R}^{B \times W}$	Matrix of ambient bin representatives; rows are $x_j^{\text{amb}}$ .
$B \in \mathbb{N}$	Total number of ambient bins (often $B = \prod_{\ell=1}^W B_{x(\ell)}$ ).
$B_\theta, B_v, B_{TI} \in \mathbb{N}$	Numbers of bins for ambient direction, speed, turbulence.
$x \in \mathbb{R}^w$	Local (at-turbine) condition vector (e.g., $\theta, v, TI$ ).
$w \in \mathbb{N}$	Number of selected local variables.
$\mathbf{X} \in \mathbb{R}^{N_T \times B \times w}$	Tensor of local (per-turbine, per-bin) wind conditions.
$x_{ij} = \mathbf{X}(i, j, :) \in \mathbb{R}^w$	Local condition at turbine $i$ , ambient bin $j$ .
$u(x) \in \mathbb{R}^{N_u}$	Control setpoint vector for local condition $x$ .
$N_u \in \mathbb{N}$	Number of control channels.
$U \in \mathbb{R}^{N_T \times B \times N_u}$	Operational plan tensor; entries $u_{ijm}$ (for $N_u=1$ , $u_{ij}$ ).
$N_T \in \mathbb{N}$	Number of turbines.
$i, j, m$	Indices for turbine, ambient bin, control channel.
$f^{\text{wake}}(\cdot)$	Wake model mapping from ambient bins and controls to local conditions.
$\mathbf{X}(U)$	Local-condition tensor from wake model under plan $U$ .
$x_j^{\text{amb}}$	Ambient vector at ambient bin $j$ .
$x_{ij}(U)$	Local condition at turbine $i$ , bin $j$ under plan $U$ .
fm	Failure mode index (e.g., tower bm, blade flapwise, blade edgewise).
$\mathcal{F}$	Set of considered failure modes.
$d_{\text{fm}}(x, u)$	Surrogate damage rate [1/h] for failure mode fm.
$P(x, u)$	Surrogate power model [W].
$h \in \mathbb{R}^B$	Lifetime frequency vector over ambient bins; $\sum_{j=1}^B h_j = H_{\text{total}}$ .
$h_j$	Expected hours in ambient bin $j$ .
$H_{\text{total}}$	Total time horizon in hours.
$p \in \mathbb{R}^B$	Ambient-bin probabilities; $\sum_{j=1}^B p_j = 1$ .
$H$	Alternative horizon (hours) used with $p$ via $h_j = H p_j$ .
$E_i(U; h)$	Lifetime energy of turbine $i$ under plan $U$ [Wh].
$D_{\text{fm}, i}(U; h)$	Lifetime damage for failure mode fm on turbine $i$ .
$F(U; h)$	Objective function (e.g., total farm energy).
$u_{\min}, u_{\max}$	Control box bounds.



Symbol	Meaning
$\theta^{\text{amb}}, v^{\text{amb}}$	Ambient wind direction [deg], speed [m/s].
$v, TI$	Local wind speed [m/s], turbulence intensity [-].
$u = \delta^P$	Derating control setpoint (percentage of rated power).
$\theta$	Local wind direction [deg].
$TI^{\text{amb}}$	Ambient turbulence intensity [-].
$\rho$	Air density [kg/m <sup>3</sup> ].
$\delta^P$	Derating factor (0–1 or %).
$\Delta^P \in \mathbb{R}^{N_T \times B}$	Derating-only operational plan; entries $\delta_{ij}^P$ .
$\delta_{ij}^P$	Derating setpoint for turbine $i$ in ambient bin $j$ .
$B_{\theta^{\text{amb}}}, B_{v^{\text{amb}}}$	Numbers of bins for ambient direction and speed.
$\Delta^{P,(k)}$	Derating plan at iteration $k$ (loop approach).
$K$	Number of loop iterations.
$\mathbf{X}^{(k)}$	Local-condition tensor at iteration $k$ .
$x_{ij}^{(k)}$	Local condition for turbine $i$ , bin $j$ , at iteration $k$ .
$\widehat{\Delta^P}$	Final derating plan after loop.
$\hat{\mathbf{X}}$	Final local-condition tensor under $\widehat{\Delta^P}$ .
$\tau_{\text{fm},i}(\Delta^P; h)$	Implied lifetime [years] of turbine $i$ for failure mode fm.
$Y^{\text{life}}$	Farm lifetime in full years (minimum across all turbines/modes).
$NPV(Y)$	Net present value over $Y$ years.
$C_{\text{elPrice}}$	Average electricity price [€/kWh].
$E^{\text{annual}}(\Delta^P; h)$	Annual energy [Wh] under plan $\Delta^P$ .
$C_{\text{OPEX}}$	Annual OPEX [€].
$C_{\text{WACC}}$	Weighted average cost of capital (discount rate) [-].
$B_{\text{opt}}, B_{\text{eval}}$	Total ambient bins for optimization/evaluation.
$h^{\text{opt}}, h^{\text{eval}}$	Frequency vectors for optimization/evaluation.
$\Delta^{P,\text{nom}}$	Nominal plan (e.g., all entries 100%).
$\tau_{\text{target}}^{\text{tower}}$	Target lifetime [years] for tower failure mode.
$D_{\text{target}}^{\text{tower}}$	Target fatigue budget for tower failure mode [-].
$y$	Yaw misalignment setpoint [deg] (if used as a control channel).
$d_{\text{flap}}, d_{\text{edge}}, d_{\text{tower}}$	Damage rates for flapwise, edgewise, and tower bm.